Gastroenterology 2015;148:427–439

BASIC AND TRANSLATIONAL—PANCREAS

Alcohol Disrupts Levels and Function of the Cystic Fibrosis Transmembrane Conductance Regulator to Promote Development of Pancreatitis

József Maléth,[1] Anita Balázs,[1] Petra Pallagi,[1] Zsolt Balla,[1] Balázs Kui,[1] Máté Katona,[1] Linda Judák,[1,2] István Németh,[3] Lajos V. Kemény,[1] Zoltán Rakonczay Jr,[1] Viktória Venglovecz,[2] Imre Földesi,[4] Zoltán Pető,[5] Áron Somorácz,[6] Katalin Borka,[6] Doranda Perdomo,[7] Gergely L. Lukacs,[7] Mike A. Gray,[8] Stefania Monterisi,[9] Manuela Zaccolo,[9] Matthias Sendler,[10] Julia Mayerle,[10] Jens-Peter Kühn,[11] Markus M. Lerch,[10] Miklós Sahin-Tóth,[12] and Péter Hegyi[1,13]

[1]First Department of Medicine, [2]Department of Pharmacology and Pharmacotherapy, [3]Department of Dermatology and Allergology, [4]Department of Laboratory Medicine, and [5]Department of Emergency Medicine, University of Szeged, Szeged, Hungary; [6]Second Department of Pathology, Semmelweis University, Budapest, Hungary; [7]Department of Physiology, McGill University, Montreal, Quebec, Canada; [8]Institute for Cell & Molecular Biosciences, Newcastle University, Newcastle upon Tyne, England; [9]Department of Physiology, Anatomy and Genetics, Oxford University, Oxford, England; [10]Department of Medicine A, University Medicine Greifswald, Greifswald, Germany; [11]Institute of Radiology, University Medicine, Ernst Moritz University, Greifswald, Germany; [12]Department of Molecular and Cell Biology, Henry M. Goldman School of Dental Medicine, Boston University, Boston, Massachusetts; and [13]MTA-SZTE Lendület Translational Gastroenterology Research Group, Szeged, Hungary

See Covering the Cover synopsis on page 267.

BACKGROUND & AIMS: Excessive consumption of ethanol is one of the most common causes of acute and chronic pancreatitis. Alterations to the gene encoding the cystic fibrosis transmembrane conductance regulator (*CFTR*) also cause pancreatitis. However, little is known about the role of CFTR in the pathogenesis of alcohol-induced pancreatitis. **METHODS:** We measured CFTR activity based on chloride concentrations in sweat from patients with cystic fibrosis, patients admitted to the emergency department because of excessive alcohol consumption, and healthy volunteers. We measured CFTR levels and localization in pancreatic tissues and in patients with acute or chronic pancreatitis induced by alcohol. We studied the effects of ethanol, fatty acids, and fatty acid ethyl esters on secretion of pancreatic fluid and HCO_3^-, levels and function of CFTR, and exchange of Cl^- for HCO_3^- in pancreatic cell lines as well as in tissues from guinea pigs and CFTR knockout mice after administration of alcohol. **RESULTS:** Chloride concentrations increased in sweat samples from patients who acutely abused alcohol but not in samples from healthy volunteers, indicating that alcohol affects CFTR function. Pancreatic tissues from patients with acute or chronic pancreatitis had lower levels of CFTR than tissues from healthy volunteers. Alcohol and fatty acids inhibited secretion of fluid and HCO_3^-, as well as CFTR activity, in pancreatic ductal epithelial cells. These effects were mediated by sustained increases in concentrations of intracellular calcium and adenosine 3′,5′-cyclic monophosphate, depletion of adenosine triphosphate, and depolarization of mitochondrial membranes. In pancreatic cell lines and pancreatic tissues of mice and guinea pigs, administration of ethanol reduced expression of *CFTR* messenger RNA, reduced the stability of CFTR at the cell surface, and disrupted folding of CFTR at the endoplasmic reticulum. CFTR knockout mice given ethanol or fatty acids developed more severe pancreatitis than mice not given ethanol or fatty acids. **CONCLUSIONS:** Based on studies of human, mouse, and guinea pig pancreata, alcohol disrupts expression and localization of the CFTR. This appears to contribute to development of pancreatitis. Strategies to increase CFTR levels or function might be used to treat alcohol-associated pancreatitis.

Keywords: Exocrine Pancreas; Cl^- Channel; Alcoholism; Duct.

Acute pancreatitis (AP) is the most common cause of hospitalization for nonmalignant gastrointestinal diseases in the United States, with an estimated annual cost of at least $2.5 billion.[1] The mortality of the disease is unacceptably high, and no specific pharmaceutical therapy is currently available. Therefore, there is a pressing economic and clinical need to develop new therapies for patients with AP.

Immoderate alcohol consumption is one of the most common causes of AP and chronic pancreatitis (CP),[1–3] and therefore the effects of ethanol and ethanol metabolites on the pancreas have been widely investigated.[4,5] However, these studies have focused mainly on pancreatic acinar and stellate cells. On the other hand, Pallagi et al showed that the initial lesion in the course of pancreatic damage during alcohol-induced chronic calcifying pancreatitis is the formation of

Abbreviations used in this paper: **AP, acute pancreatitis; ATP, adenosine triphosphate; ATPase, adenosine triphosphatase; $(ATP)_i$, intracellular adenosine triphosphate; BAC, blood alcohol concentration; $[Ca^{2+}]_i$, intracellular Ca^{2+} concentration; cAMP, adenosine 3′,5′-cyclic monophosphate; CF, cystic fibrosis; CFTR, cystic fibrosis transmembrane conductance regulator; Cl^-_{sw}, sweat Cl^- concentration; CP, chronic pancreatitis; ER, endoplasmic reticulum; H_2DIDS, dihydro-4,4′-diisothiocyanostilbene-2,2′-disulfonic acid; IP_3R, inositol triphosphate receptor; KO, knockout; mRNA, messenger RNA; PDEC, pancreatic ductal epithelial cell; PA, palmitic acid; POA, palmitoleic acid; POAEE, palmitoleic acid ethyl ester; Tg, thapsigargin; WT, wild-type.**

0016-5085/$36.00
http://dx.doi.org/10.1053/j.gastro.2014.11.002

mucoprotein plugs in the small pancreatic ducts.[6] These changes are very similar to the alterations of the exocrine pancreas in cystic fibrosis (CF), the most common autosomal recessive disease caused by loss-of-function mutations in the *CFTR* gene. Moreover, Ratcliff et al showed that patients with CF who have impaired cystic fibrosis transmembrane conductance regulator (CFTR) function are at increased risk for developing pancreatitis.[7] These data suggest that changes in the function or expression of the CFTR Cl^- channels in pancreatic ductal epithelial cells (PDECs), which alone express CFTR in the exocrine pancreas,[8] may play a central role in the pathogenesis of alcohol-induced pancreatitis.

Patients and Methods

Detailed protocols and descriptions of the volunteers, patients, and methods used in this study are provided in Supplementary Methods.

Human Studies

Sweat samples from human subjects were collected by pilocarpine iontophoresis, and sweat chloride concentration was determined by conductance measurement. The messenger RNA (mRNA) and protein expression levels of CFTR and Na^+/K^+–adenosine triphosphatase (ATPase) of the pancreatic ductal epithelia in human pancreatic tissue were determined.

Cell and Animal Studies

A large variety of human cell lines (Capan-1, MDCK, and HEK) and animal models (mice and guinea pigs) were used to assess the role of CFTR in alcohol-induced AP.

Statistical Analysis

All data are expressed as means ± SEM. Significant differences between groups were determined by analysis of variance. Statistical analysis of the immunohistochemical data was performed using the Mann–Whitney *U* test. $P < .05$ was considered statistically significant.

Ethical Approvals

The protocols concerning human subjects or laboratory animals were approved by the relevant agencies.

Results

Alcohol Consumption Decreases CFTR Activity and Expression in Human Subjects

In patients with CF, sweat Cl^- concentration (Cl^-_{sw}) is elevated due to diminished CFTR absorptive activity.[9] In our study, Cl^-_{sw} at 0 mmol/L blood alcohol concentration (BAC) was 41.08 ± 3.1 mmol/L (Figure 1*A*). After consuming 1.6 g/kg ethanol within 30 minutes, the average BAC was elevated to 23.3 ± 1.1 mmol/L, with no elevation of Cl^-_{sw} (47 ± 1 mmol/L). However, to test the effects of higher BAC on Cl^-_{sw}, we enrolled patients admitted to the emergency department because of excessive alcohol consumption. The average BAC in this group was 74.2 ± 2.6 mmol/L but the Cl^-_{sw} was 62.7 ± 2.3 mmol/L, suggesting strong inhibition of CFTR (Figure 1*B*; for patient data, see Supplementary Table 2). Importantly, when the BAC returned to 0, the Cl^-_{sw} normalized (Figure 1*C*). To assess the effects of long-term alcohol intake, we also enrolled alcohol-dependent patients from the department of addictology. These patients had a history of alcohol consumption for at least 1 year and did not consume alcohol for at least 1 week before measurement of Cl^-_{sw}. The mean Cl^-_{sw} in this group was 49.92 ± 2.8 mmol/L, suggesting that alcohol has long-term effects on CFTR as well (Figure 1*B*).

Next, we determined the effects of alcohol on CFTR expression and localization in the pancreas using tissue samples from control pancreatic tissue and from patients with acute or chronic alcohol-induced pancreatitis (Figure 1*D–F*; for a detailed description of tissue samples, see Supplementary Methods). In alcoholic AP, CFTR expression decreased at both mRNA and protein levels. Similarly, in CP, membrane expression of CFTR in PDECs was significantly lower; however, both the mRNA level and cytoplasmic density of CFTR were strongly elevated, suggesting defective endoplasmic reticulum (ER) protein folding and/or translocation of CFTR from the membrane to the cytosol. As a control experiment, we showed that neither mRNA nor protein expression levels of another plasma membrane transporter, namely Na^+/K^+-ATPase, were changed in AP and CP (Supplementary Figure 1).

Ethanol and Fatty Acid Impair Pancreatic Fluid and Bicarbonate Secretion and Inhibit CFTR Cl^- Channel Activity In Vivo and In Vitro

In the next step, we applied different in vivo and in vitro techniques to assess the effects of ethanol and ethanol metabolites on pancreatic fluid and HCO_3^- secretion in animal models and in a human pancreatic cell line. First, we used magnetic resonance imaging cholangiopancreatography to measure total excreted volume in wild-type (WT) and CFTR knockout (KO) mice. On retro-orbital injection of 10 U/kg body weight secretin, the increase in total excreted volume in WT animals was significantly higher than in CFTR KO animals (Figure 2*A*). Pancreatic secretion was reassessed 24 hours after intraperitoneal injection of 1.75 g/kg ethanol and 750 mg/kg palmitic acid (PA). The total excreted volume was markedly decreased in WT mice and almost completely abolished in CFTR KO mice. In addition, we showed that intraperitoneal injection of ethanol and PA significantly decreased both basal and secretin-stimulated pancreatic fluid secretion in anesthetized mice in vivo (Supplementary Figure 2).

To detect pancreatic ductal fluid secretion in vitro, we used isolated guinea pig pancreatic ducts, which is the best in vitro model to mimic the human situation. Administration of 100 mmol/L ethanol or the nonoxidative ethanol metabolite palmitoleic acid (POA; 200 μmol/L) for 30 minutes markedly reduced pancreatic fluid secretion, whereas 200 μmol/L palmitoleic acid ethyl ester (POAEE) had no effect (Figure 2*B*). Pancreatic ductal HCO_3^- secretion was measured using NH_4Cl pulse, where the initial rate of intracellular pH recovery from an alkali load (base flux; $J[B^-]$; for details, see Supplementary Methods) reflects the

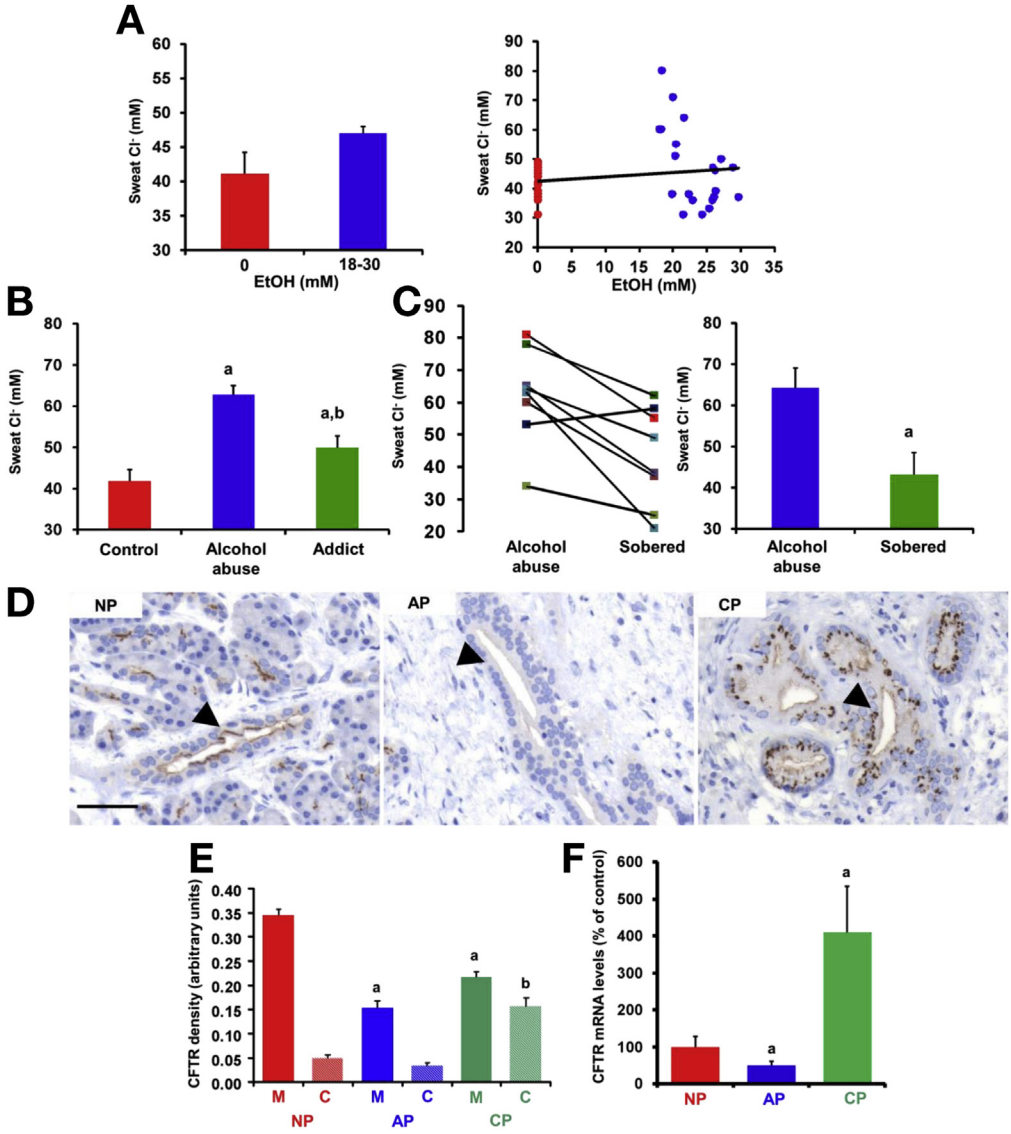

Figure 1. Alcohol consumption decreases activity and expression of the CFTR Cl^- channel. (*A*) No significant change in Cl^-_{sw} was observed in healthy volunteers (n = 21) before and after ethanol consumption. (*B*) Cl^-_{sw} was significantly higher in patients after excessive alcohol consumption (EAC) compared with age- and sex-matched controls, whereas it was elevated in alcoholic subjects with 0 mmol/L BAC (Addict) compared with the control group but significantly lower than in the alcohol abuse group. Control, n = 26; EAC, n = 49; Addict, n = 15. $^aP < 0.001$ vs control, $^bP < .001$ vs EAC. (*C*) The Cl^-_{sw} of patients returned to a normal level when measured several days after EAC at 0 mmol/L BAC. n = 8. $^aP < .001$ vs EAC values. (*D* and *E*) CFTR expression in human pancreas. *Arrowheads* point to the luminal membrane of the intralobular pancreatic ducts. NP, normal pancreas. *Scale bar* = 50 μm. CFTR staining density at the luminal membrane was decreased in both acute and chronic pancreatitis (AP and CP), whereas cytoplasmic density was markedly increased in CP. C, cytoplasm; M, membrane. n = 5/group. $^aP < .05$ vs NP-M, $^bP < .05$ vs NP-C. (*F*) Quantitative polymerase chain reaction analysis of CFTR mRNA expression in human pancreas. CFTR mRNA levels were decreased in AP and highly increased in CP (normalized to 18 ribosomal RNA; given as percentage of NP mRNA). n = 5/group. $^aP < .05$ vs NP.

activity of the apical SLC26 Cl^-/HCO_3^- exchangers and CFTR (Figure 2*C*).[10] Similarly to ductal fluid secretion, 100 mmol/L ethanol and 200 μmol/L POA significantly diminished ductal HCO_3^- secretion after 30 minutes of exposure.

We confirmed our results on a human polarized pancreatic cell line (Capan-1) as well. Applying 2 independent methods (luminal Cl^- removal and NH_4Cl pulse) showed that 15-minute administration of a low concentration of ethanol (10 mmol/L) stimulated a high concentration of ethanol (100 mmol/L) and POA (100, 200 μmol/L) significantly impaired the apical Cl^-/HCO_3^- exchange activity (Supplementary Figure 3*A*). Moreover, 100 mmol/L ethanol and 100 to 200 μmol/L POA significantly inhibited the recovery from acid load during NH_4Cl pulse experiments under basal conditions and forskolin stimulation (Supplementary Figure 3*B–D*), suggesting that activity of the basolateral transporters may be also impaired.

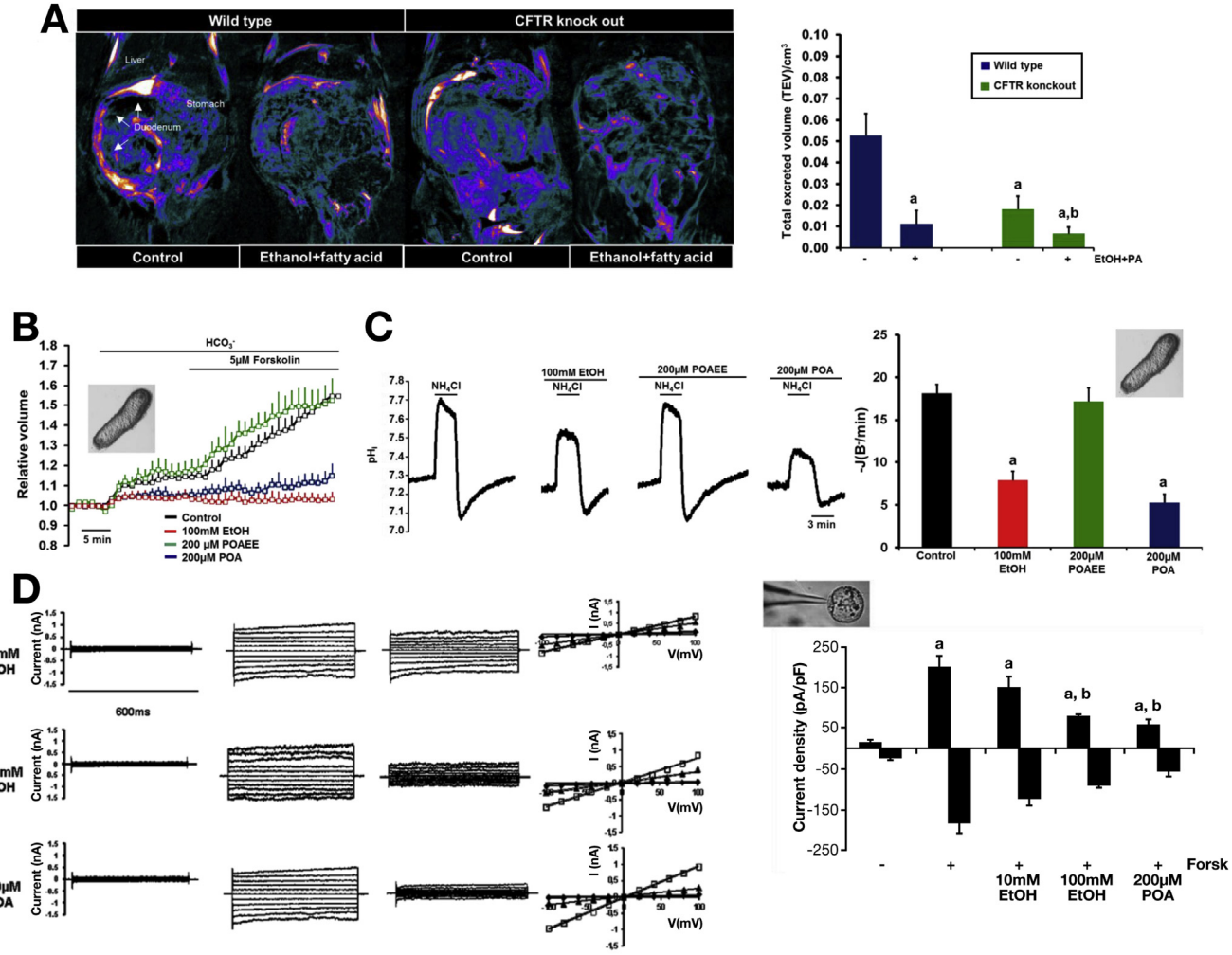

Figure 2. Ethanol and fatty acids inhibit pancreatic fluid and HCO_3^- secretion and CFTR Cl^- current. (*A*) Reconstructed images of duodenal filling after secretin stimulation. Compared with WT, duodenal filling was significantly reduced in CFTR KO mice and was abolished after intraperitoneal injection of ethanol plus palmitic acid (PA). n = 6/group. $^aP < .05$ vs WT control, $^bP < .05$ vs KO control. (*B*) Changes in the relative luminal volume of isolated guinea pig pancreatic ducts show that administration of ethanol and POA but not POAEE for 30 minutes diminished in vitro ductal fluid secretion. n = 3–4 experiments/group. (*C*) Measurement of luminal Cl^-/HCO_3^- exchange activity shows that basolateral administration of 100 mmol/L ethanol and 200 μmol/L POA significantly inhibited activity of the luminal SLC26 Cl^-/HCO_3^- exchanger and CFTR and decreased recovery from the alkali load in isolated guinea pig pancreatic ducts. n = 3–5 experiments/group. $^aP < .05$ vs control. (*D*) Representative fast whole cell CFTR Cl^- current recordings in guinea pig pancreatic ductal cells. *Left to Right:* Unstimulated currents, currents after forskolin stimulation (10 μmol/L; 10 minutes), stimulated currents after 10 minutes of treatment, and current-voltage relationships (*diamonds*, unstimulated; *squares*, forskolin stimulated; *triangles*, forskolin-stimulated currents after treatment). The summary of the current densities (pA/pF; measured at reversal potential: ±60 mV) show that 100 mmol/L ethanol or 200 μmol/L POA blocked the forskolin-stimulated CFTR Cl^- currents (61.5% ± 5.15% and 73.1% ± 4.46%, respectively). n = 5–6/group. $^aP < .05$ vs basal current, $^bP < .05$ vs forskolin-stimulated current.

Finally, we directly detected the effects of ethanol and ethanol metabolites on the CFTR Cl^- current in primary epithelial (Figure 2*D*) and human Capan-1 cells (Supplementary Figure 3*E*). Exposure of guinea pig PDECs to 10 mmol/L ethanol had no significant effect on forskolin-stimulated CFTR currents (in Capan-1, significant slight stimulation was observed), whereas 100 mmol/L ethanol or 200 μmol/L POA caused a significant decrease. In both cases, inhibition was voltage independent and irreversible. Administration of 200 μmol/L POAEE had no effect on forskolin-stimulated CFTR currents.

Low Concentration of Ethanol Stimulates Both the Apical SLC26 Cl^-/HCO_3^- Exchanger and CFTR via Inositol Triphosphate Receptor–Mediated Ca^{2+} Signaling

Apical Cl^- removal in Capan-1 cells revealed that separate administration of 10 μmol/L CFTR(inh)-172 (CFTR Cl^- channel inhibitor) or 500 μmol/L dihydro-4,4′-diisothiocyanostilbene-2,2′-disulfonic acid (H_2DIDS) (SLC26A6 inhibitor) for 15 minutes could not prevent the stimulatory effect of 10 mmol/L ethanol; however, their combination

totally abolished it (Supplementary Figure 4*A* and *C*). In case of NH_4Cl pulse (where the bicarbonate concentration of the cells is higher), not only coadministration of the 2 inhibitors but also separate administrations alone could prevent the stimulatory effect of ethanol (Supplementary Figure 4*B* and *D*). To identify the intracellular mechanisms of stimulation, we showed that 10 mmol/L ethanol induced repetitive Ca^{2+} spikes in Capan-1 cells (Supplementary Figure 5*A*). Administration of the inositol triphosphate receptor (IP_3R) antagonist caffeine (20 mmol/L) or the phospholipase C inhibitor U73122 (10 μmol/L) completely abolished the Ca^{2+} response, suggesting that Ca^{2+} was released from the ER via activation of IP_3R. Moreover, 20 mmol/L caffeine totally inhibited the stimulatory effect of ethanol, suggesting that elevation of intracellular Ca^{2+} concentration ($[Ca^{2+}]_i$) mediates the stimulatory effect of ethanol on HCO_3^- secretion (Supplementary Figure 5*B* and *C*).

High Concentration of Ethanol Inhibits Both the Apical SLC26 Cl^-/HCO_3^- Exchanger and CFTR

Administration of CFTR(inh)-172 and H_2DIDS showed that pretreatment of cells for 15 minutes with either CFTR(inh)-172 or H_2DIDS further decreased HCO_3^- secretion when coadministrated with ethanol or POA, suggesting that both transport mechanisms are involved in inhibitory mechanisms (Figure 3*A* and *B* and Supplementary Figure 6*A* and *B*). When the SLC26

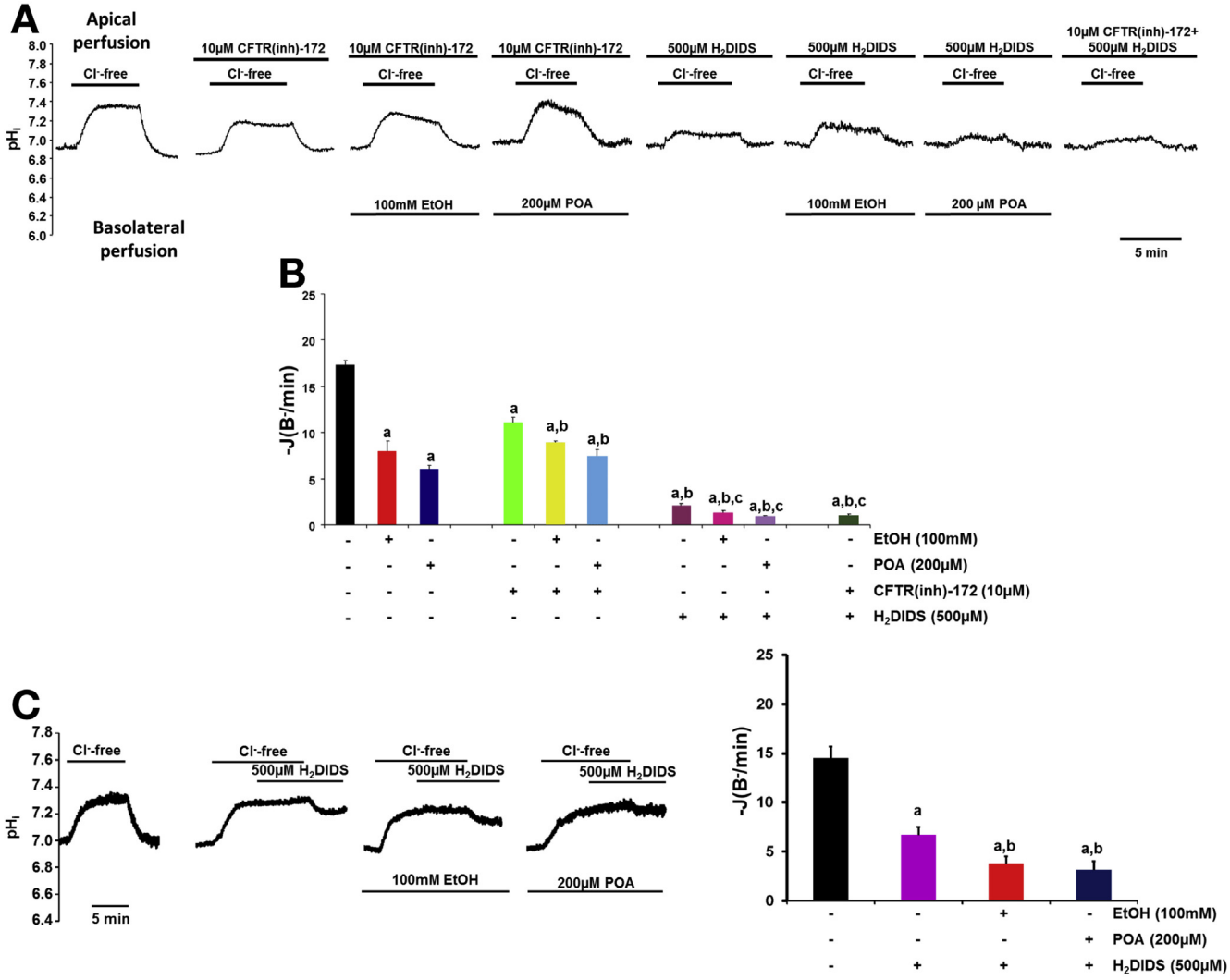

Figure 3. Ethanol and POA inhibit both the luminal Cl^-/HCO_3^- exchanger and CFTR in Capan-1 cells. (*A* and *B*) The initial rate of intracellular pH (pH_i) recovery after luminal Cl^- readdition shows the effects of basolateral administration of 100 mmol/L ethanol or 200 μmol/L POA in the presence or absence of 500 μmol/L H_2DIDS and/or 10 μmol/L CFTR(inh)-172 (luminal administration). (*Labels above the traces*, composition of the luminal solution; *labels below the traces*, composition of the basolateral solution.) A total of 100 mmol/L ethanol and 200 μmol/L POA induced further inhibition after administration of CFTR(inh)-172 and/or H_2DIDS, suggesting that high concentrations of ethanol and POA inhibit the activity of CBE and CFTR on the apical membrane of PDECs. $^aP < .05$ vs control, $^bP < .05$ vs 10 μmol/L CFTR(inh)-172, $^cP < .05$ vs 500 μmol/L H_2DIDS. (*C*) Representative pH_i traces and summary data of the initial rate of pH_i recovery after Cl^- readdition using a different protocol confirmed our results. $^aP < .05$ vs control, $^bP < .05$ vs 500 microM H2DIDS. n = 3–5 experiments for all groups.

inhibitor H_2DIDS was administered only when the luminal Cl^- was already removed (Figure 3*C*), the same effects were observed.

High Concentrations of Ethanol and POA Induce Sustained Elevation of $[Ca^{2+}]_i$, Decreased Mitochondrial Function and Adenosine 3′,5′-Cyclic Monophosphate Level

Ethanol (100 mmol/L) induced a moderate but sustained increase in $[Ca^{2+}]_i$ in Capan-1 cells, POAEE had no effect, and POA evoked a dose-dependent, sustained increase in $[Ca^{2+}]_i$ (Figure 4*A* and *B*). The first phase of the Ca^{2+} signal was inhibited by the ryanodine receptor inhibitor Ruthenium Red, the IP_3R inhibitor caffeine, and the phospholipase C inhibitor U73122 (Supplementary Figure 7*A*), whereas removal of extracellular Ca^{2+} had no effect on the $\Delta Ratio_{max}$ (Supplementary Figure 7*B*). The plateau phase of the signal was totally dependent on the presence of extracellular Ca^{2+} and blocked by gadolinium, suggesting the involvement of the store-operated Ca^{2+} channels. To verify that 200 μmol/L POA completely depletes the ER Ca^{2+} stores, we administered POA in Ca^{2+}-free media followed by administration of 2 μmol/L thapsigargin (Tg; sarcoplasmic/ER calcium ATPase [SERCA] inhibitor). Under these conditions, Tg was not able to induce further Ca^{2+} release (Supplementary Figure 8*A*). For control, we administered Tg before POA, where POA had no effect on $[Ca^{2+}]_i$. These data indicate that POA completely depletes the ER Ca^{2+} stores and induces extracellular Ca^{2+} influx.

To further characterize the effects of POA on extracellular Ca^{2+} influx, we performed the Tg-Ca^{2+} readdition protocol[11] (Supplementary Figure 8*B* and *C*). Treatment with Tg depleted ER Ca^{2+} and readdition of extracellular Ca^{2+} evoked store-operated Ca^{2+} influx, where the steady state is maintained by plasma membrane Ca^{2+}-ATPase activity. POA (200 μmol/L) in Ca^{2+}-free extracellular solution mimicked the effect of Tg (depleted the ER Ca^{2+} store and induced store-operated Ca^{2+} entry). However, after the store-operated Ca^{2+} entry–mediated increase in Ca^{2+}, the decrease in $[Ca^{2+}]_i$ was markedly slower than in the case of Tg-treated cells and the plateau was reached on an elevated $[Ca^{2+}]_i$. These results suggest that POA not only depletes ER Ca^{2+} but also decreases plasma membrane Ca^{2+}-ATPase activity.

Measurement of intracellular adenosine triphosphate $[(ATP)_i]$ using Magnesium Green AM (Life Technologies; Grand Island, NY) revealed that 100 mmol/L ethanol and 100 to 200 μmol/L POA markedly and irreversibly decreased $(ATP)_i$ (Figure 4*B*). (The increase in fluorescent intensity inversely correlates with the cellular adenosine triphosphate [ATP] levels.) The combination of deoxyglucose/iodoacetate/carbonyl cyanide 3-chlorophenylhydrazone was used as control to inhibit cellular glycolysis and mitochondrial ATP production. We also tested the effect of $(ATP)_i$ depletion on HCO_3^- secretion (Supplementary Figure 9*C* and *D*) and showed that administration of deoxyglucose/iodoacetate/carbonyl cyanide 3-chlorophenylhydrazone significantly decreased HCO_3^- secretion, similarly to the effects of 200 μmol/L POA. To further characterize the effects of ethanol and ethanol metabolites on mitochondrial function, we showed that 100 mmol/L ethanol and 100 to 200 μmol/L POA markedly and irreversibly decreased mitochondrial membrane potential $[(\Delta\Psi)_m]$ (Figure 4*C*). FRET-based adenosine 3′,5′-cyclic monophosphate (cAMP) measurements using Epac1-camps sensor revealed that 100 mmol/L ethanol and 200 μmol/L POAEE significantly decreased forskolin-stimulated cAMP production in HEK cells; however, interestingly, 100 μmol/L POA had no inhibitory effect (Figure 4*D*). Finally, we showed that chelation of intracellular Ca^{2+} (with 40 μmol/L 1,2-bis(o-aminophenoxy)ethane-*N*,*N*,*N*′,*N*′-tetraacetic acid [BAPTA-AM]) completely abolished the inhibitory effect of 100 mmol/L ethanol and 200 μmol/L POA on pancreatic ductal HCO_3^- secretion, suggesting that it was mediated by the sustained elevation of $[Ca^{2+}]_i$ (Figure 4*E* and Supplementary Figure 9*A* and *B*).

Ethanol and Nonoxidative Ethanol Metabolites Cause Translocation and Expression Defect of CFTR

Our experiments showed that high concentrations of ethanol, POAEE, and POA time- and dose-dependently decreased both mRNA and protein expression of CFTR in human pancreatic epithelial cells in vitro (Figure 5*A*–*C*). To reproduce these observations in vivo, an appropriate animal model was used. Guinea pigs were injected intraperitoneally with 0.8 g/kg ethanol and 300 mg/kg PA. Importantly, apical CFTR expression in the pancreatic ducts was not changed at 3 and 6 hours; however, it was significantly decreased 12 and 24 hours after treatment (Figure 5*E* and *F*). Moreover, cytoplasmic CFTR levels were elevated after 3 hours, suggesting a membrane trafficking defect of CFTR. As a control experiment, expression of Na^+/K^+-ATPase was also measured and no changes were observed (Supplementary Figure 10).

Ethanol and Its Metabolites Decrease CFTR Expression and Plasma Membrane Density via Accelerated Channel Plasma Membrane Turnover and Damaged Protein Folding

To dissect the mechanism of CFTR expression defect on ethanol, POA, or POAEE exposure, we exposed monolayers of MDCK-II cells expressing WT human CFTR containing a 3HA epitope in the fourth extracellular loop to ethanol, POAEE, or POA for 48 hours. Quantitative immunoblot analysis by anti-HA antibody revealed that in contrast to the modest effect of 100 mmol/L ethanol, 100 to 200 μmol/L POAEE and POA significantly decreased mature, complex glycosylated CFTR expression as compared with control (Figure 6*A*). Importantly, protein expression of Na^+/K^+-ATPase did not change during treatment. Loss of cellular CFTR expression coincided with reduction of apical CFTR plasma membrane density, monitored by the cell surface enzyme-linked immunosorbent assay taking advantage of the extracellular 3HA epitope (Figure 6*B*). CFTR apical plasma membrane density was reduced by ~40% in the

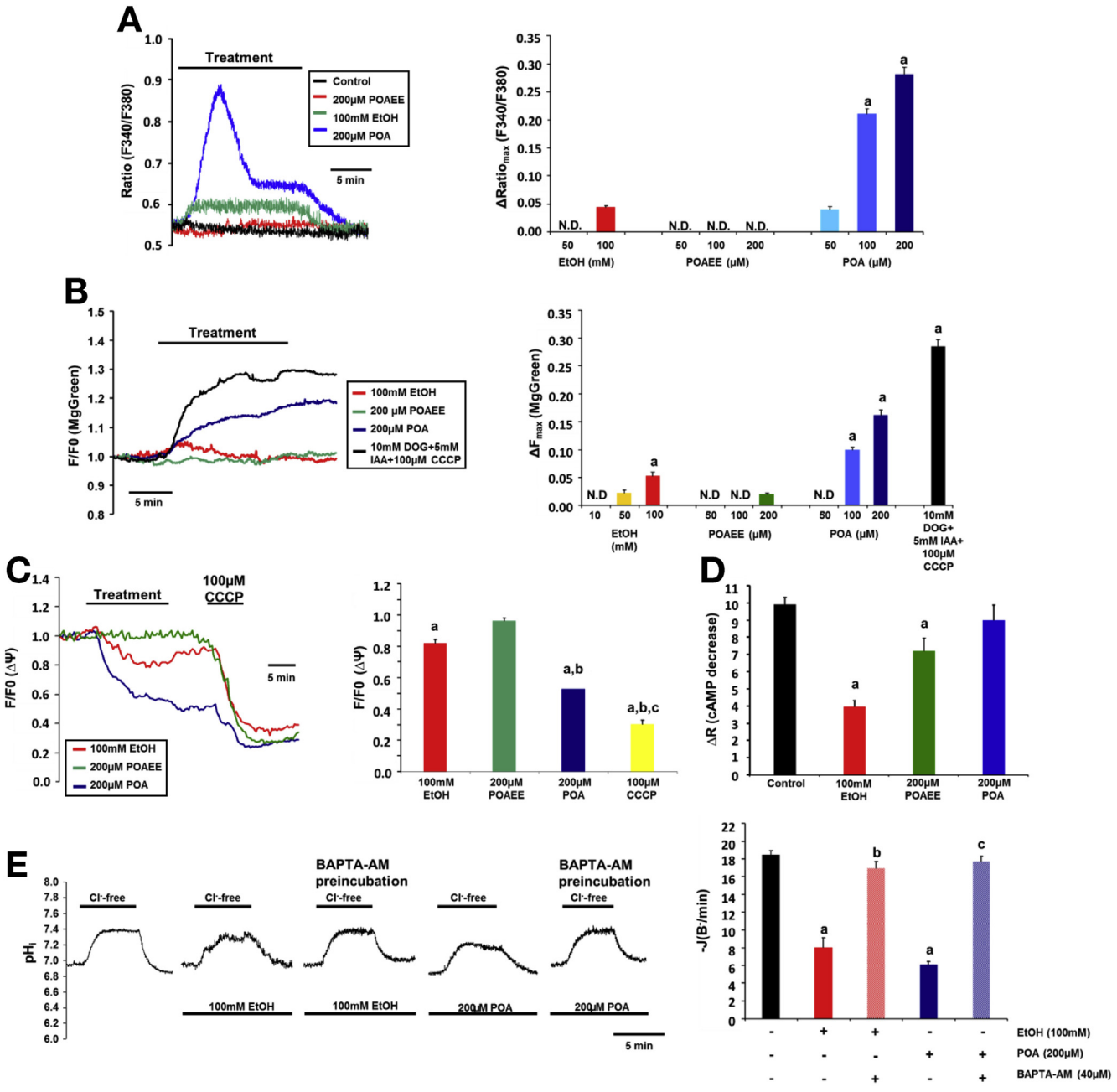

Figure 4. High concentrations of ethanol and POA induce sustained elevation of $[Ca^{2+}]_i$, impaired mitochondrial function, and decreased cAMP levels in Capan-1 PDECs. (*A*) Representative traces and summary data of the $\Delta Ratio_{max}$ show the effect of ethanol, POAEE, and POA on $[Ca^{2+}]_i$. Ethanol (100 mmol/L) induced a small, sustained elevation of $[Ca^{2+}]_i$, whereas 100 to 200 μmol/L POA induced a significantly higher increase in $[Ca^{2+}]_i$. $^aP < .05$ vs 100 mmol/L ethanol. (*B*) Ethanol and POA induced significant and irreversible depletion of $(ATP)_i$. Deoxyglucose/iodoacetic acid (DOG/IAA; glycolysis inhibition) and CCCP (inhibition of mitochondrial ATP production) served as control. (*C*) Representative traces and summary data of changes in the mitochondrial membrane potential [$(\Delta\Psi)$m]. Ethanol (100 mmol/L) induced a moderate decrease in $(\Delta\Psi)$m, whereas 200 μmol/L POA had a more prominent effect. CCCP induced a further decrease in $(\Delta\Psi)$m after treatment with POA. (*D*) Summary data for cAMP measurements. A total of 100 mmol/L ethanol and 200 μmol/L POAEE significantly decreased forskolin-stimulated cAMP production. (*E*) Ca^{2+} chelation abolished the inhibitory effect of ethanol and POA on intracellular pH recovery after luminal Cl^- readdition. For all conditions, n = 3–5/group. $^aP < .05$ vs control; $^bP < .05$ vs 100 mmol/L ethanol; $^cP < .05$ vs 200 μmol/L POA. N.D., not detected.

presence of 200 μmol/L POA, while only ~15% and ~30% was evident after ethanol and POAEE exposure, respectively (Figure 6*C*). Accelerated channel turnover at the plasma membrane and/or impaired biosynthetic secretion can account for the pronounced apical expression defect of CFTR in treated cells. To assess the first possibility, apical plasma membrane stability of CFTR was measured by enzyme-linked immunosorbent assay, which revealed that

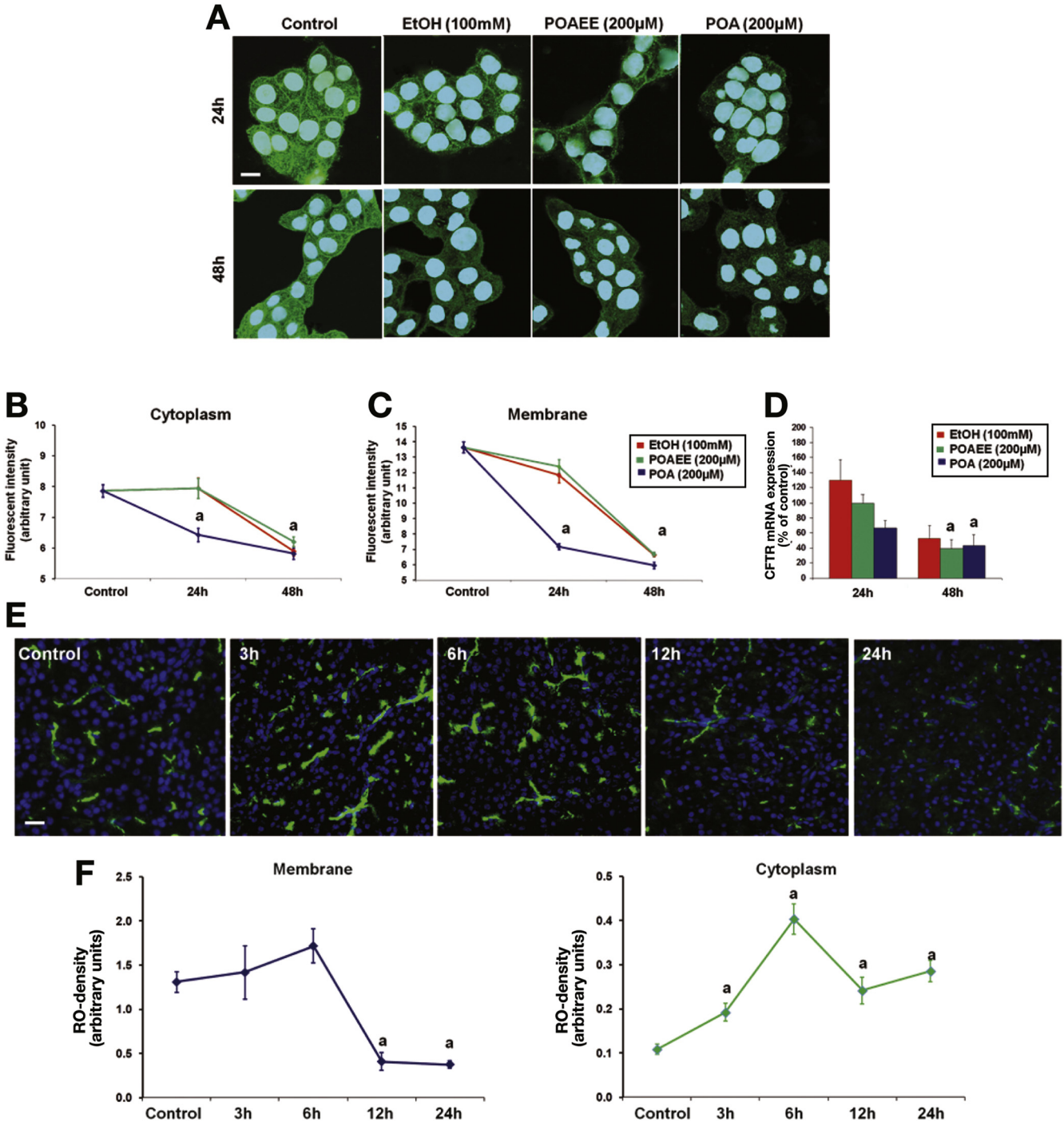

Figure 5. Ethanol, POAEE, and POA decrease CFTR expression in Capan-1 cells and in guinea pig pancreatic ducts. (*A–C*) High concentrations of ethanol, POAEE, and POA induced a significant decrease in CFTR membrane and cytoplasmic protein expression. *Scale bar* = 10 μm. (*D*) Ethanol, POAEE, and POA decreased CFTR mRNA expression after 48 hours of exposure. Data were normalized to HPRT mRNA levels and expressed as percentage of untreated control mRNA levels. (*E* and *F*) CFTR expression in guinea pig pancreas. Expression of CFTR on the luminal membrane of guinea pig pancreatic ducts was significantly decreased 12 hours after a single intraperitoneal injection of 0.8 g/kg ethanol and 300 mg/kg PA. *Scale bar* = 100 μm. n = 5/group. $^{a}P < .05$ vs control.

ethanol, POAEE, and POA provoked increased removal of CFTR from the plasma membrane during a 2-hour chase, suggesting that channel turnover was accelerated (Figure 6*C*). The conformational maturation efficiency of CFTR was measured by the conversion efficiency of the metabolically labeled core glycosylated form into the complex glycosylated CFTR (Figure 6*D*). CFTR folding efficiency was diminished from 24% ± 3% to 17% ± 2% and 20% ± 1% by POA and POAEE, respectively (Figure 6*D*), indicating that nonoxidative ethanol metabolites compromise both the

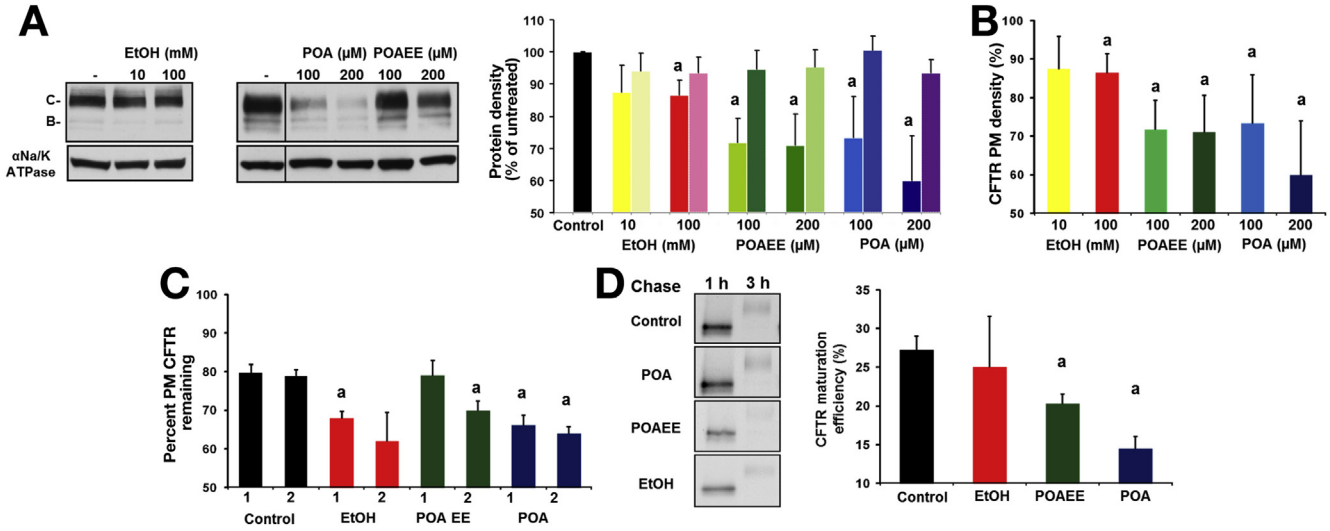

Figure 6. Effect of ethanol and its metabolites on CFTR and Na^+/K^+-ATPase expression. (*A*) Immunoblotting and densitometry of CFTR and Na^+/K^+-ATPase expression levels in transfected MDCK monolayers after 48 hours of treatment with ethanol, POA, or POAEE (*right panel*). Results are expressed as percentage of the complex glycosylated CFTR (*band C*) or Na^+/K^+-ATPase expression in untreated cells (control). (*First column*, CFTR; *second column*, Na^+/K^+-ATPase for each condition.) (*B*) Enzyme-linked immunosorbent assay measurement of the apical plasma membrane (PM) density of CFTR revealed that ethanol, POA, and POAEE decreased this parameter after 48 hours of incubation. Results are presented as percentage of CFTR cell surface density of the untreated cells. (*C*) Ethanol, POAEE, and POA reduce the PM stability of CFTR determined by cell surface enzyme-linked immunosorbent assay. Cell surface resident CFTR was labeled with anti-HA antibody and chased for 1 or 2 hours in the presence of the indicated compounds at 37°C. Results are presented as percentage of the initial CFTR surface density (*1* and *2* indicate 1-hour and 2-hour chase, respectively). (*D*) CFTR folding efficiency was reduced by 100 mmol/L ethanol and diminished by 200 μmol/L POA or POAEE after 48 hours. CFTR folding efficiency was calculated as the percentage of the pulse-labeled, core glycosylated form converted into the mature complex glycosylated form during 3-hour chase. n = 3 for each condition. $^aP < .05$ vs control.

biosynthetic processing and peripheral stability of the channel.

Genetic Deletion of CFTR Increases the Severity of Alcohol-Induced Pancreatitis

To further confirm the central role of CFTR in alcohol-induced pancreatic damage, we compared the severity of alcohol- and PA-induced pancreatitis in WT and CFTR KO mice. Intraperitoneal administration of 1.75 g/kg ethanol and 750 mg/kg PA induced significant elevation of all investigated parameters of severity of pancreatitis (pancreatic water content, serum amylase activity, edema score, leukocyte score, and necrosis) (Figure 7*A* and *B*) in WT animals. Importantly, these alterations were significantly higher in CFTR KO animals, showing that when expression and activity of CFTR is impaired by alcohol abuse, alcohol-induced AP worsens.

Discussion

In this study, we showed that ethanol and its nonoxidative metabolites cause impairment of CFTR function and expression, which exacerbate alcohol-induced pancreatitis (Supplementary Figure 11). Although a single binge of alcohol in healthy volunteers did not impair CFTR function as determined by sweat chloride absorption, excessive alcohol consumption in habitual drinkers markedly reduced the function of CFTR, as evidenced by a rise in Cl^-_{sw}, which returned to the normal range when the measurement was repeated on sobered patients.

Pancreatic tissue metabolizes ethanol mainly via the nonoxidative pathway mediated by FAEE synthases, which combine ethanol and FA and produce FAEE.[12] A clinical study showed that blood FAEE concentration was elevated in parallel with ethanol concentration during alcohol consumption, but FAEE remained increased longer in serum compared with ethanol.[13] Moreover, compared with the liver, pancreatic FAEE synthases activity is higher, which creates the possibility of local accumulation of nonoxidative ethanol metabolites.[14] Werner et al[15] showed that infusion of FAEE induced pancreatic edema, intrapancreatic trypsinogen activation, and vacuolization of acinar cells. Recently, Huang et al[16] developed a novel model of alcohol-induced pancreatitis using combined intraperitoneal injection of ethanol and FA, in which the pharmacological inhibition of nonoxidative ethanol metabolism decreased pancreatic damage.

We showed that pancreatic ductal HCO_3^- secretion plays a central role in the physiology of the exocrine pancreas, maintaining intraductal pH[17,18]; therefore, in our experiments, we used different in vivo and in vitro techniques to clarify the short-term effects of ethanol and ethanol metabolites on fluid and HCO_3^- secretion and CFTR Cl^- current in PDECs. Importantly, our magnetic resonance imaging cholangiopancreatography experiments showed that ductal

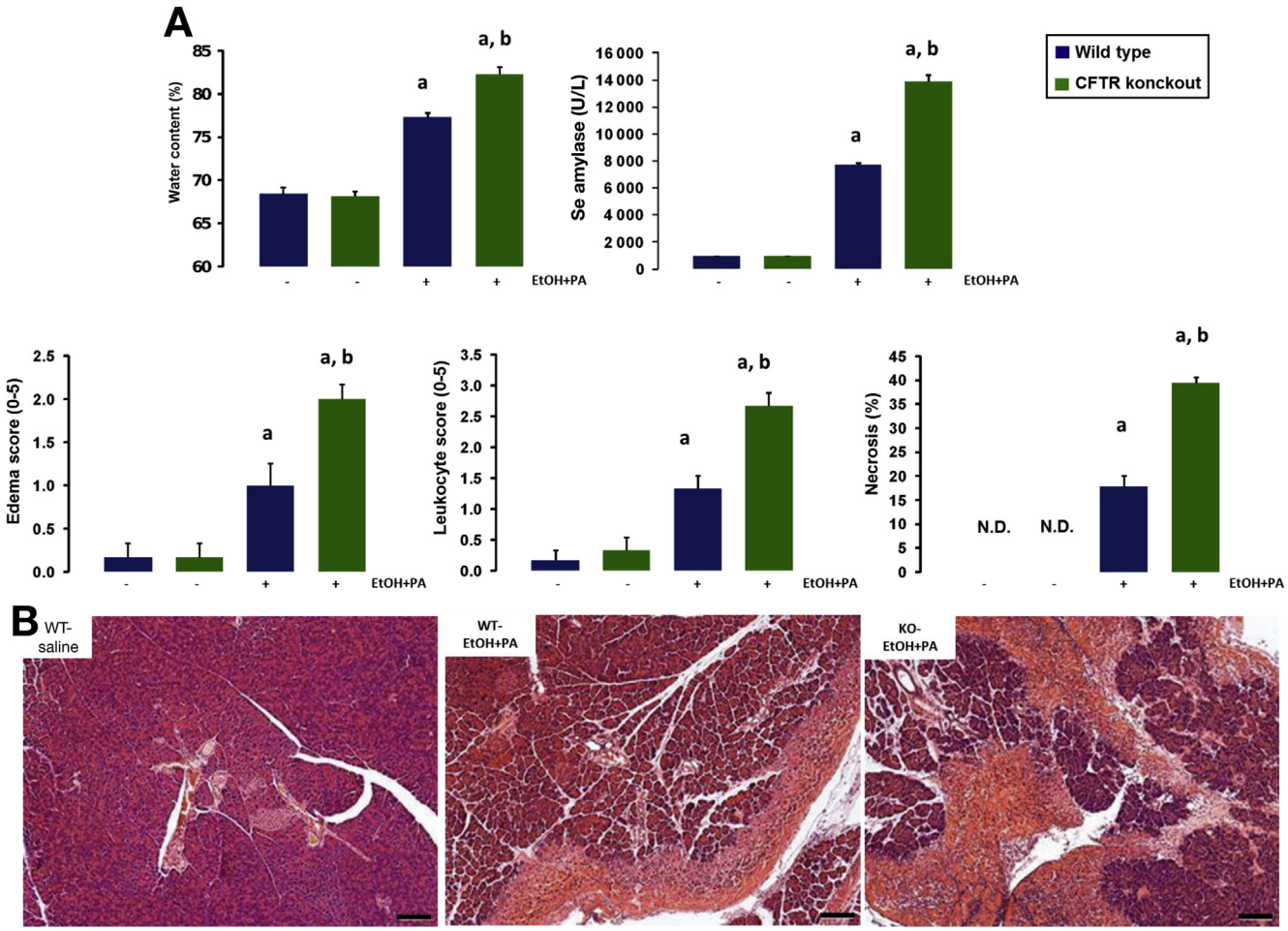

Figure 7. AP induced by ethanol and fatty acids is more severe in CFTR KO mice. (*A*) Induction of AP by a single intraperitoneal injection of ethanol and PA induced significant elevation of pancreatic water content as measured by 100 * (wet weight − dry weight)/wet weight), serum amylase activity, edema and leukocyte scores, and necrosis. The severity of pancreatitis was significantly higher in CFTR KO mice. (*B*) Representative H&E-stained light micrographs of pancreas sections from WT control and ethanol + PA–treated WT or CFTR KO mice. Note the massive necrosis in the treated animals. *Scale bars* = 100 μm. Data are shown as means ± SEM. $^{a}P < .05$ vs control, $^{b}P < .05$ vs WT ethanol + PA–treated group. n = 6/group. N.D., not detected.

secretion is remarkably diminished in CFTR KO mice compared with WT; moreover, ethanol and PA strongly impaired ductal secretion in both groups. The inhibitory effect of ethanol and PA on pancreatic fluid secretion was confirmed in vivo using pancreatic duct cannulation in anesthetized mice and in vitro using isolated sealed guinea pig pancreatic ducts as well. Besides fluid transport, we characterized the effects of ethanol and its metabolites on HCO_3^- secretion. Our results showed that ethanol in low concentrations stimulates and in high concentrations inhibits HCO_3^- secretion and decreases CFTR activity. Similar dual effects of ethanol on fluid secretion were highlighted earlier.[19] In our study, the stimulatory effect of 10 mmol/L ethanol on HCO_3^- secretion was mediated by IP_3R-dependent Ca^{2+} release from the ER. In contrast, high concentrations of ethanol and POA induced sustained $[Ca^{2+}]_i$ elevation mediated by both IP_3R and ryanodine receptor as well as extracellular Ca^{2+} influx (Figure 7*C*). Notably, similar toxic Ca^{2+} elevation was found in pancreatic acinar cells and other cell types, leading to premature protease activation and cell death.[20–23] It is well documented that sustained $[Ca^{2+}]_i$ elevation causes mitochondrial Ca^{2+} overload,[24] which impairs $(\Delta\Psi)_m$ and ATP production.[20,25] Very recently ethanol was shown to sensitize pancreatic mitochondria to activate the mitochondrial permeability transition pore, leading to mitochondrial failure.[26] In this study, high concentrations of ethanol and POA also induced depletion of intracellular ATP and decreased $(\Delta\Psi)_m$. Although the toxic effects of ethanol and POA were similar to those of a high concentration of bile acids,[27,28] in this study chelation of $[Ca^{2+}]_i$ abolished the inhibitory effect of ethanol and POA on HCO_3^- secretion. This observation indicates that ethanol and POA, in a similar manner to trypsin,[29] inhibit HCO_3^- secretion via a sustained increase in $[Ca^{2+}]_i$. Importantly, CFTR single channel parameters do not change as a result of use of ethanol (personal communication, June, 2013; Aleksandrov Andrei and John R. Riordan), suggesting that

the effects of a high dose of ethanol do not alter the biophysical characteristics of CFTR.

One of the crucial observations of this study is that expression of CFTR is decreased on the luminal membrane of human PDECs during alcohol-induced pancreatitis. Because decreased CFTR expression during alcoholic pancreatitis is very similar to the CFTR mislocalization found in autoimmune pancreatitis,[30] we wanted to confirm that decreased CFTR expression is caused by alcohol and not by cellular damage during the inflammatory process. The in vitro experiments in human PDECs and the in vivo experiments in guinea pigs clearly showed that alcohol and its nonoxidative metabolites indeed strongly decrease CFTR expression without pancreatitis. The pronounced apical expression defect of CFTR was caused by accelerated channel turnover at the plasma membrane and impaired biosynthetic secretion (Figure 7*C*). The latter effect may be attributed, at least in part, to chronic cytoplasmic ATP depletion, considering that CFTR conformation maturation is an ATP-sensitive process at the ER.[31] These results indicate that long-term exposure of PDECs to ethanol or ethanol metabolites compromise both the biosynthetic processing and peripheral stability of the channel. It is known that the phosphorylation and dephosphorylation of CFTR mediated by WNK/SPAK and IRBIT/PP1 regulates the plasma membrane trafficking of CFTR and other transporters in epithelial cells[32,33]; however, the effect of ethanol or ethanol metabolites on these systems is not known. Long-term alcohol consumption dose-dependently increases the risk of developing malignancies, diabetes, hypertension, and cardiovascular diseases.[34] Interestingly, Guo et al[35] showed that CFTR activity plays a crucial role in insulin secretion of pancreatic beta cells, whereas diabetes is a well-known complication of alcoholism.[34] The decreased CFTR activity induced by alcohol consumption might play an important role in disease development.

The association between *CFTR* gene mutations and the risk of development of recurrent AP[36] or CP[37] provides strong evidence that mutations in *CFTR* and/or insufficiency of electrolyte and fluid secretion by pancreatic ductal cells lead to an increased risk of pancreatitis.[38] Heterozygous carriers of *CFTR* mutations are at increased risk for CP[39]; moreover, Ooi et al[7] showed that the risk of developing pancreatitis was much higher in patients with CF, who had milder *CFTR* mutations (type IV and V) and were pancreatic sufficient compared with those who had severe mutations and were pancreatic insufficient. In the pathogenetic model proposed in this study, the risk of developing pancreatitis inversely correlates with CFTR function. However, in other studies, the association between *CFTR* gene mutation and alcoholic pancreatitis was inconsistent.[40,41] Very recently, LaRusch et al elegantly showed that *CFTR* gene mutations that do not cause typical CF but disrupt the WNK1-SPAK–mediated HCO_3^- permeability of the channel are associated with pancreatic disorders.[42] In an animal model of pancreatitis, DiMagno et al earlier showed that CFTR KO mice developed more severe AP after cerulein hyperstimulation than WT mice.[43] Pallagi et al recently had the same observation in mice with genetic deletion of Na^+/H^+ exchanger regulatory factor (NHERF1), which regulates CFTR expression.[44] Here we have shown with CFTR KO mice that genetic deletion of CFTR leads to more severe pancreatitis after ethanol and fatty acid administration, confirming the crucial role of CFTR in the pathogenesis of alcohol-induced pancreatitis.

Taken together, our observations provide evidence that loss of CFTR function not only plays a crucial role in *CFTR* mutation–related pancreatitis but also contributes to the pathogenesis of alcohol-induced pancreatitis. These data indicate that correcting CFTR function should offer therapeutic benefit in AP.

Supplementary Material

Note: To access the supplementary material accompanying this article, visit the online version of *Gastroenterology* at www.gastrojournal.org and at http://dx.doi.org/10.1053/j.gastro.2014.11.002.

References

1. Yadav D, Lowenfels AB. The epidemiology of pancreatitis and pancreatic cancer. Gastroenterology 2013;144:1252–1261.
2. Nagar AB, Gorelick FS. Acute pancreatitis. Curr Opin Gastroenterol 2002;18:552–557.
3. Braganza JM, Lee SH, McCloy RF, et al. Chronic pancreatitis. Lancet 2011;377:1184–1197.
4. Pandol SJ, Lugea A, Mareninova OA, et al. Investigating the pathobiology of alcoholic pancreatitis. Alcohol Clin Exp Res 2011;35:830–837.
5. Petersen OH, Tepikin AV, Gerasimenko JV, et al. Fatty acids, alcohol and fatty acid ethyl esters: toxic Ca2+ signal generation and pancreatitis. Cell Calcium 2009;45:634–642.
6. Sarles H, Sarles JC, Camatte R, et al. Observations on 205 confirmed cases of acute pancreatitis, recurring pancreatitis, and chronic pancreatitis. Gut 1965;6:545–559.
7. Ooi CY, Dorfman R, Cipolli M, et al. Type of CFTR mutation determines risk of pancreatitis in patients with cystic fibrosis. Gastroenterology 2011;140:153–161.
8. Trezise AE, Buchwald M. In vivo cell-specific expression of the cystic fibrosis transmembrane conductance regulator. Nature 1991;353:434–437.
9. Siegenthaler P, Dehaller R, Dubach UC. Salt excretion in sweat in cystic fibrosis. JAMA 1963;186:1178.
10. Hegyi P, Gray MA, Argent BE. Substance P inhibits bicarbonate secretion from guinea pig pancreatic ducts by modulating an anion exchanger. Am J Physiol Cell Physiol 2003;285:C268–C276.
11. Bird GS, DeHaven WI, Smyth JT, et al. Methods for studying store-operated calcium entry. Methods 2008;46:204–212.
12. Laposata EA, Lange LG. Presence of nonoxidative ethanol metabolism in human organs commonly damaged by ethanol abuse. Science 1986;231:497–499.

13. Doyle KM, Cluette-Brown JE, Dube DM, et al. Fatty acid ethyl esters in the blood as markers for ethanol intake. JAMA 1996;276:1152–1156.
14. Gukovskaya AS, Mouria M, Gukovsky I, et al. Ethanol metabolism and transcription factor activation in pancreatic acinar cells in rats. Gastroenterology 2002; 122:106–118.
15. Werner J, Laposata M, Fernandez-del Castillo C, et al. Pancreatic injury in rats induced by fatty acid ethyl ester, a nonoxidative metabolite of alcohol. Gastroenterology 1997;113:286–294.
16. **Huang W, Booth DM**, Cane MC, et al. Fatty acid ethyl ester synthase inhibition ameliorates ethanol-induced Ca^{2+}-dependent mitochondrial dysfunction and acute pancreatitis. Gut 2014;63:1313–1324.
17. Hegyi P, Petersen OH. The exocrine pancreas: the acinar-ductal tango in physiology and pathophysiology. Rev Physiol Biochem Pharmacol 2013;165:1–30.
18. Hegyi P, Maleth J, Venglovecz V, et al. Pancreatic ductal bicarbonate secretion: challenge of the acinar acid load. Front Physiol 2011;2:36.
19. Yamamoto A, Ishiguro H, Ko SB, et al. Ethanol induces fluid hypersecretion from guinea-pig pancreatic duct cells. J Physiol 2003;551:917–926.
20. Criddle DN, Murphy J, Fistetto G, et al. Fatty acid ethyl esters cause pancreatic calcium toxicity via inositol trisphosphate receptors and loss of ATP synthesis. Gastroenterology 2006;130:781–793.
21. Kouzoukas DE, Li G, Takapoo M, et al. Intracellular calcium plays a critical role in the alcohol-mediated death of cerebellar granule neurons. J Neurochem 2013;124: 323–335.
22. Nakayama N, Eichhorst ST, Muller M, et al. Ethanol-induced apoptosis in hepatoma cells proceeds via intracellular Ca(2+) elevation, activation of TLCK-sensitive proteases, and cytochrome c release. Exp Cell Res 2001;269:202–213.
23. Kruger B, Albrecht E, Lerch MM. The role of intracellular calcium signaling in premature protease activation and the onset of pancreatitis. Am J Pathol 2000;157:43–50.
24. Kroemer G, Reed JC. Mitochondrial control of cell death. Nat Med 2000;6:513–519.
25. Walsh C, Barrow S, Voronina S, et al. Modulation of calcium signalling by mitochondria. Biochim Biophys Acta 2009;1787:1374–1382.
26. Shalbueva N, Mareninova OA, Gerloff A, et al. Effects of oxidative alcohol metabolism on the mitochondrial permeability transition pore and necrosis in a mouse model of alcoholic pancreatitis. Gastroenterology 2013; 144:437–446 e6.
27. Maleth J, Venglovecz V, Razga Z, et al. Non-conjugated chenodeoxycholate induces severe mitochondrial damage and inhibits bicarbonate transport in pancreatic duct cells. Gut 2011;60:136–138.
28. Maleth J, Rakonczay Z Jr, Venglovecz V, et al. Central role of mitochondrial injury in the pathogenesis of acute pancreatitis. Acta Physiol (Oxf) 2013;207: 226–235.
29. Pallagi P, Venglovecz V, Rakonczay Z Jr, et al. Trypsin reduces pancreatic ductal bicarbonate secretion by inhibiting CFTR Cl(-) channels and luminal anion exchangers. Gastroenterology 2011;141:2228–2239 e6.
30. **Ko SB, Mizuno N**, Yatabe Y, et al. Corticosteroids correct aberrant CFTR localization in the duct and regenerate acinar cells in autoimmune pancreatitis. Gastroenterology 2010;138:1988–1996.
31. Lukacs GL, Mohamed A, Kartner N, et al. Conformational maturation of CFTR but not its mutant counterpart (delta F508) occurs in the endoplasmic reticulum and requires ATP. EMBO J 1994;13:6076–6086.
32. Yang D, Li Q, So I, et al. IRBIT governs epithelial secretion in mice by antagonizing the WNK/SPAK kinase pathway. J Clin Invest 2011;121:956–965.
33. Park S, Hong JH, Ohana E, et al. The WNK/SPAK and IRBIT/PP1 pathways in epithelial fluid and electrolyte transport. Physiology (Bethesda) 2012;27:291–299.
34. Shield KD, Parry C, Rehm J. Chronic diseases and conditions related to alcohol use. Alcohol Res 2013; 35:155–173.
35. Guo JH, Chen H, Ruan YC, et al. Glucose-induced electrical activities and insulin secretion in pancreatic islet beta-cells are modulated by CFTR. Nat Commun 2014;5:4420.
36. Cavestro GM, Zuppardo RA, Bertolini S, et al. Connections between genetics and clinical data: Role of MCP-1, CFTR, and SPINK-1 in the setting of acute, acute recurrent, and chronic pancreatitis. Am J Gastroenterol 2010;105:199–206.
37. **Weiss FU, Simon P**, Bogdanova N, et al. Complete cystic fibrosis transmembrane conductance regulator gene sequencing in patients with idiopathic chronic pancreatitis and controls. Gut 2005;54:1456–1460.
38. Hegyi P, Rakonczay Z. Insufficiency of electrolyte and fluid secretion by pancreatic ductal cells leads to increased patient risk for pancreatitis. Am J Gastroenterol 2010;105:2119–2120.
39. Sharer N, Schwarz M, Malone G, et al. Mutations of the cystic fibrosis gene in patients with chronic pancreatitis. N Engl J Med 1998;339:645–652.
40. Maruyama K, Harada S, Yokoyama A, et al. Association analyses of genetic polymorphisms of GSTM1, GSTT1, NQO1, NAT2, LPL, PRSS1, PSTI, and CFTR with chronic alcoholic pancreatitis in Japan. Alcohol Clin Exp Res 2010;34(suppl 1):S34–S38.
41. Pezzilli R, Morselli-Labate AM, Mantovani V, et al. Mutations of the CFTR gene in pancreatic disease. Pancreas 2003;27:332–336.
42. **LaRusch J, Jung J, General IJ**, et al. Mechanisms of CFTR functional variants that impair regulated bicarbonate permeation and increase risk for pancreatitis but not for cystic fibrosis. PLoS Genet 2014;10: e1004376.
43. Dimagno MJ, Lee SH, Hao Y, et al. A proinflammatory, antiapoptotic phenotype underlies the susceptibility to acute pancreatitis in cystic fibrosis transmembrane regulator (-/-) mice. Gastroenterology 2005;129: 665–681.
44. **Pallagi P, Balla Z, Singh AK**, et al. The role of pancreatic ductal secretion in protection against acute pancreatitis in mice. Crit Care Med 2014;42:e177–e188.

Author names in bold designate shared co-first authorship.

Received March 18, 2014. Accepted November 4, 2014.

Reprint requests
Address requests for reprints to: Péter Hegyi, MD, PhD, DSc, First Department of Medicine, Faculty of Medicine, University of Szeged, Korányi fasor 8-10, H-6720 Szeged, Hungary. e-mail: hegyi.peter@med.u-szeged.hu; fax: (36) 62-545-185.

Acknowledgments
The authors thank John Riordan (University of North Carolina at Chapel Hill) and Cystic Fibrosis Foundation Therapeutics for providing the CFTR antibody, Ursula Seidler (Department of Gastroenterology, Hannover Medical School) for the kind gift of the CFTR knockout mice, Éva Kereszthy (Department of Forensic Medicine, University of Szeged) for legal advice concerning investigation of alcoholic patients, Erzsébet Schneider and coworkers in the emergency unit of the Second Department of Medicine (University of Szeged) for help with measurements in alcohol-intoxicated patients and the volunteers participating in our study, and the 1st Department of Surgery (Semmelweis University) for providing surgical resection samples.

Conflicts of interest
The authors disclose no conflicts.

Funding
Supported by MTA-SZTE Momentum Grant (LP2014-10/2014), by the Hungarian National Development Agency (TÁMOP-4.2.2.A-11/1/KONV-2012-0035, TÁMOP-4.2.2-A-11/1/KONV-2012-0052, TÁMOP-4.2.2.A-11/1/KONV-2012-0073, TÁMOP-4.2.4.A/2-11-1-2012-0001, TÁMOP-4.2.4.A2-SZJÖ-TOK-13-0017) and the Hungarian Scientific Research Fund (NF100677). M.M.L. was supported by grants from the Alfried Krupp von Bohlen und Halbach Foundation (Graduate Schools of Tumour Biology and Free Radical Biology), the Deutsche Krebshilfe/Dr Mildred Scheel Stiftung (109102), the Deutsche Forschungsgemeinschaft (DFG GRK840-E3/E4, DFG GRK1947, MA 4115/1-2/3), the Federal Ministry of Education and Research (BMBF GANI-MED 03152061A and BMBF 0314107, 01ZZ9603, 01ZZ0103, 01ZZ0403, 03ZIK012), and the European Union (EU-FP-7: EPC-TM and EU-FP7-REGPOT-2010-1, EPC-TM-Net). MS-T was supported by the National Institutes of Health (NIH) grant R01 DK058088.

Supplementary Methods

Solutions and Chemicals

Supplementary Table 1 summarizes the composition of the solutions used in these series of experiments. The pH of the HEPES-buffered solutions was set to 7.4 with HCl, whereas the HCO_3^--buffered solutions were gassed with 95% o_2/5% co_2 to set pH. For patch clamp studies, the standard extracellular solution contained (in mmol/L) 145 NaCl, 4.5 KCl, 2 $CaCl_2$, 1 $MgCl_2$, 10 HEPES, and 5 glucose (pH 7.4). The osmolarity of the external solutions was 300 mOsm/L. The standard pipette solution contained (in mmol/L) 120 CsCl, 2 $MgCl_2$, 0.2 ethylene glycol-bis(β-aminoethyl ether)-*N*,*N*,*N*′,*N*′-tetraacetic acid (EGTA), 10 HEPES, and 1 Na_2ATP (pH 7.2). 2,7-bis-(2-carboxyethyl)-5-(and-6-)carboxyfluorescein-acetoxymethy lester (BCECF-AM), 2-(6-(bis(carboxymethyl)amino)-5-(2-(2-(bis(carboxymethyl)amino)-5-methylphenoxy)ethoxy)-2-benzofuranyl)-5-oxazolecarboxylic-acetoxymethylester (Fura2-AM), Magnesium Green-AM, tetramethylrhodamine methyl ester (TMRM), H_2DIDS, and 1,2-bis(o-aminophenoxy)ethane-*N*,*N*,*N*′,*N*′-tetraacetic acid (BAPTA-AM) were from Invitrogen (Carlsbad, CA). Forskolin was purchased from Tocris (Ellisville, MO) and Tg from Merck (Darmstadt, Germany). All other chemicals were obtained from Sigma-Aldrich (Budapest, Hungary) unless stated otherwise. To solubilize fatty acids in water-based solution, first we made 1 mol/L stock solution of POA and POAEE in 100% ethanol. Then, 10 μL stock solution was added carefully to 1 mL HEPES or HCO_3^-/co_2 buffered solution at 37°C, which was gently sonicated. This was then added dropwise and diluted to the concentration used during the experiments again at 37°C. In this way, we were able to avoid using a high concentration of ethanol.

Human Studies

Characteristics of volunteers and patients. Detailed characteristics of the volunteers and alcohol intoxicated patients enrolled in the study are summarized in Supplementary Table 2. All volunteers were healthy. Patients were admitted to the emergency department for excessive alcohol consumption but did not have acute or chronic disease. Smokers were not enrolled in this study because cigarette smoke itself can decrease CFTR function.[1] The laboratory parameters (Supplementary Table 2, including markers of fluid loss) of the 2 groups were not significantly different and were within normal limits except the serum sodium level, which was slightly elevated in the alcohol intoxicated patients. It has been shown that excessive alcohol consumption can alter thermoregulatory responses and thermal sensations during mild heat exposure in humans and can increase skin blood flow and sweating.[2] On the other hand, long-term alcohol consumption has been shown to alter the autonomic nervous system, which might decrease sweat production.[3] In our experiments, we did not experience any changes in sweat response to pilocarpine stimulation.

Collection of sweat samples. Pilocarpine iontophoresis was conducted according to the method of Gibson and Cooke[4] using the Macroduct system (Wescor, Logan, UT). Cl^-_{sw} was determined by conductance measurement using the Wescor Sweat-Chek 3100.

Collection of serum samples. Simultaneously with the sweat test, 5 mL of blood was drawn into a native yellow tube. After coagulation, the samples were centrifuged (3000 RCF, 10 minutes, 4°C) and stored at −20°C. Serum alcohol levels were measured by routine laboratory test.

Determination of the effect of ethanol on Cl^-_{sw} in a self-controlled experiment. Studies were conducted on 21 healthy volunteers. Subjects were asked to refrain from ethanol intake 24 hours before the experiment. Blood samples were taken before (−45 minutes) and after (90, 120, 240, 300 minutes) alcohol consumption, whereas sweat samples were taken before and 90 minutes after alcohol consumption. Ethanol intake was calculated using the updated Widmark's formula[5] for each subject.

Genotyping R117H and ΔF508 variants of CFTR. Genomic DNA was isolated from 300 μL EDTA blood using the QIAamp DNA Blood Mini Kit (Qiagen, Hilden, Germany). Primers were designed according to the genomic sequence of CFTR on chromosome 7 (GenBank: NC_000007.14) (see primer sequences in Supplementary Table 3). Polymerase chain reaction (PCR) was performed in a total volume of 30 μL, which contained 0.5 U HotStarTaq DNA Polymerase (Qiagen), 1.5 mmol/L $MgCl_2$, 0.2 mmol/L deoxynucleoside triphosphate, 0.5 μmol/L of each primer, and 10 to 50 ng genomic DNA. Amplification was performed under the following cycle conditions: 95°C for 5 minutes to activate the enzyme, followed by 35 cycles of 30-second denaturation at 95°C, 30-second annealing at 60°C, and 1-minute extension at 72°C, with a final extension of 5 minutes. The R117H variant was genotyped by sequencing. ΔF508 PCR products were analyzed on a 10% native polyacrylamide gel and electrophoresed for 3 hours at 80 V. To visualize DNA fragments, the gel was stained with ethidium bromide for 10 minutes. Good resolution of normal (113 base pairs) and mutant allele (110 base pairs) was achieved. None of the patients carried *CFTR* mutations (ΔF508CFTR, R117H).

Pancreatic tissue samples. Human pancreatic tissue samples were obtained from autopsy and from surgical resections. Control pancreatic tissue (n = 5) were from tumor-free tissue surrounding neuroendocrine pancreatic tumors. Tissue samples from patients with AP (n = 5) were from autopsy and from surgical resections. The average age of these patients was 56 ± 2.8 years, and the male/female ratio was 1.5:1. All patients had elevated serum lipase and liver enzyme levels and a history of alcohol consumption. Tissue samples from patients with CP (n = 5) were from surgical resections. The average age of these patients was 56.8 ± 2.8 years, and the male/female ratio was 4:1. All patients had elevated serum liver enzyme levels and a history of alcohol consumption.

Quantitative real-time reverse-transcription PCR. CFTR mRNA expression of human pancreatic tissue

was investigated using tissue samples from control patients or patients with acute or chronic alcohol-induced pancreatitis. Total RNA was isolated from three 10-μm-thick sections cut from a formalin-fixed, paraffin-embedded tissue block applying Qiagen RNeasy FFPE Kit. Total RNA (1 μg) from each sample was submitted to reverse transcription by applying the High Capacity RNA-to-cDNA kit (Applied Biosystems, Foster City, CA) according to the manufacturer's guide. Real-time PCR was performed by using ABI PRISM 7000 (Applied Biosystems) using duplicates of 100 ng complementary DNA and TaqMan Gene Expression Assay primers (catalog no. 4331182; Applied Biosystems) for CFTR (ID: Hs00357011_m1), Na^+/K^+-ATPase (ID: Hs00167556_m1), and the control gene 18S ribosomal RNA (ID: Hs99999901_s1). The expression rate was calculated by the $2^{\Delta CT}$ method.

Immunohistochemistry. Paraffin-embedded, 3- to 4-μm-thick sections of surgically removed resection specimens and autopsy tissue samples were used for immunohistochemistry. After deparaffinization of the tissue samples with EZ Prep Concentrate 10X (Ventana Medical Systems, Tucson, AZ), endogen peroxidase blocking and antigen retrieval (CC1; Ventana Medical Systems), monoclonal CFTR anti–C-terminal antibody (1:300 dilution; incubation at 42°C for 30 minutes; Millipore, Billerica, MA), anti–Na^+/K^+-ATPase (1:6000; incubation at 42°C for 30 minutes; clone H3; Santa Cruz Biotechnology, Dallas, TX) have been used. Immunohistochemical staining was performed with horseradish peroxidase multimer–based, biotin-free detection technique according to the protocol of the automated Ventana system (Ventana Benchmark XT; Ventana Medical Systems). For visualization, the UltraView Universal DAB Detection Kit (Ventana Medical Systems) was applied. Sections from human pancreas were used as positive controls. For negative control, primary antibodies were substituted with antibody diluent (Ventana Medical Systems). The stained slides were digitized with Mirax Pannoramic MIDI and Mirax Pannoramic SCAN digital slide scanners (3DHistech Ltd, Budapest, Hungary).

Calculation of relative optical density. The ImageJ program (National Institutes of Health, Bethesda, MD) was used to calculate relative optical (RO) density. Pixel values (PV) were normalized to erythrocyte density in all cases. The RO-Density value was calculated from the RO-Density $= \log_{10}(255/PV_{Norm})$ equation as described earlier, assuming that the brightest value in the image equals 255.[6]

Cell and Animal Studies

Animals, pancreatic ductal cell isolation, and cell culturing. *Mice.* CFTR knockout mice were originally generated by Ratcliff et al[7] and a kind gift of Ursula Seidler.[8] The mice were congenic on the FVB/N background. No WT CFTR protein is made by the null CF mice, because the hypoxanthine phosphoribosyltransferase (HPRT) cassette disrupts the *cftr* coding sequence and introduces a termination codon, and none of the possible RNA transcripts from the disrupted locus can encode a functional CFTR protein. Genotyping was performed by reverse-transcription PCR. The animals were kept at a constant room temperature of 24°C with a 12-hour light-dark cycle and were allowed free access to specific CFTR chow and drinking solution in the Animal Facility of the First Department of Medicine at University of Szeged. The mice received electrolyte drinking solution containing polyethylene glycol and high HCO_3^- (in mmol/L: 40 Na_2SO_4, 75 $NaHCO_3$, 10 NaCl, 10 KCl, 23 g/L^{-1} polyethylene glycol 4000), and a fiber-free diet (C1013; Altromin, Lage, Germany) to allow survival beyond weaning. All mice were genotyped before the experiments. WT refers to the +/+ littermates of the CFTR KO mice. The mice used in this study were 6 to 8 weeks old and weighed 20 to 25 g, and the sex ratio was 1:1 for all groups.

Guinea pigs. Four- to 8-week-old guinea pigs were killed by cervical dislocation, and intralobular/interlobular ducts were isolated by enzymatic digestion and microdissection from the pancreas and cultured overnight as previously described.[9] Single pancreatic ductal cells were isolated as described previously.[10]

Cell cultures. Capan-1 cells were obtained from American Type Culture Collection (HTB-79; Manassas, VA) and used for experiments between 20 and 60 passages. Cells were cultured according to the distributors' instructions. For the intracellular pH (pH_i) measurements, 5×10^5 cells were seeded onto polyester permeable supports (12-mm diameter, 0.4-mm pore size, Transwell; Corning Inc, Corning, NY). Cell confluence was checked by light microscopy and determination of transepithelial electrical resistance using an EVOM-G Volt-Ohm-Meter (World Precision Instruments, Sarasota, FL). Experiments were performed after the transepithelial electrical resistance of the monolayer increased to at least 50 Ωcm^2 (after subtraction of the filter resistance). For $[Ca^{2+}]_i$ or intracellular ATP level $[(ATP)_i]$, measurements of 5×10^5 cells were seeded onto 24-mm-diameter cover glasses and for confocal imaging to assess mitochondrial membrane potential $[(\Delta\Psi)_m]$. A total of 2.5×10^5 cells were seeded onto glass bottom dishes (MatTek, Ashland, MA) and grown until ~60% to 80% confluency.

For FRET-based cAMP measurements, HEK293 cells (American Type Culture Collection) were grown in Dulbecco modified Eagle medium (Invitrogen) supplemented with 10% fetal bovine serum (Invitrogen), L-glutamine, penicillin, and streptomycin at 37°C under 5% CO_2. Cells were plated on 24-mm glass coverslips and at 80% to 90% confluence were transiently transfected with the FRET-based sensor Epac1-camps[11] using Lipofectamine transfection reagent (Life Technologies) according to the manufacturer's protocol. FRET imaging was conducted 24 hours later. In these series of experiments, 100 μmol/L POA were used because 200 μmol/L induced immediate detachment of HEK cells from the cover glass. At the end of the experiments, supraphysiological concentrations of forskolin were added combined with 100 μmol/L 3-isobutyl-1-methylxanthine to induce a maximal increase in cAMP.

For CFTR cell surface stability and ER folding measurements, MDCK type II cells stably expressing CFTR-3HA variants under a tetracycline-responsive promoter were

generated by lentivirus transduction using the Lenti-X Tet-On Advanced Inducible Expression System (Clontech, Mountain View, CA) under puromycin (3 μg/mL) and G418 selection (0.2 mg/mL), grown in Dulbecco modified Eagle medium (Invitrogen) supplemented with 10% fetal bovine serum as specified previously.[6] For all experiments, epithelial cells were cultured at confluence for 4 days in the presence of 500 ng/mL doxycycline to induce expression of CFTR-3HA.

Magnetic resonance imaging of exocrine pancreatic fluid secretion. Magnetic resonance imaging (MRI) was performed to measure pancreatic exocrine function as described previously.[12,13] Quantification of duodenal filling after secretin stimulation was observed in 6 WT and 6 CFTR knockout mice before and 24 hours after intraperitoneal injection with a mixture of 1.75 g/kg ethanol and 750 mg/kg PA. Animals were allowed free access to pineapple juice instead of water 12 hours before the MRI examination. MRI was performed in a 7.1-Tesla animal scanner (Bruker, Ettlingen, Germany). Strong T_2-weighted series of the complete abdomen were acquired before and after retro-orbital injection of secretin (ChiroStim; ChiRho-Clin, Burtonville, MD) at a dose of 10 IU units/kg body weight. The time between injection and MRI was 6 minutes. The sequences were acquired using the following image parameters: TR/TE, 4400/83 milliseconds; flip angle, 180°; matrix, 256 × 256; field of view, 40 × 40 mm; bandwidth, 315 Hz/pixel; slice thickness, 1 mm; 20 slices. All image analyses were performed using OsiriX (version 5; Pixmeo, Geneva, Switzerland). First, we reduced image noise to minimize artifacts in images. Second, fluid excretion into the small intestine was segmented in each slice. Care was taken to avoid artifacts caused by magnetic inhomogeneity and motion, especially bowel motion. The volume of intestinal fluid was assessed before and after secretin stimulation. From these data, total extracted volume was assessed.

Measurement of pancreatic fluid secretion. *In vitro.* Fluid secretion into the closed luminal space of the cultured guinea pig pancreatic ducts was analyzed using a swelling method developed by Fernandez-Salazar et al.[14] Briefly, the ducts were transferred to a perfusion chamber (0.45 mL) and attached to a coverslip precoated with poly-L-lysine in the base of the chamber. Bright-field images were acquired at 1-minute intervals using a charge-coupled device camera (CFW 1308C; Scion Corp, Frederick, MD). The integrity of the duct wall was checked at the end of each experiment by perfusing the chamber with a hypotonic solution (standard HEPES-buffered solution diluted 1:1 with distilled water). Digital images of the ducts were analyzed using Scion Image software (Scion Corp) to obtain values for the area corresponding to the luminal space in each image.

In vivo. In vivo pancreatic fluid secretion was assessed in mice before and 24 hours after intraperitoneal injection with a mixture of 1.75 g/kg ethanol and 750 mg/kg PA. Mice were anesthetized with 1.5 g/kg urethane by intraperitoneal injection. The body temperature of the mice was maintained by placing the animals on a warm pad (37°C) during the experiments. The abdomen was opened, and the lumen of the common biliopancreatic duct was cannulated with a blunt-end 31-gauge needle. The proximal end of the common duct was then occluded with a microvessel clip to prevent contamination with bile, and the pancreatic juice was collected in a PE-10 tube for 30 minutes. Using an operating microscope, the jugular vein was cannulated for intravenous administration of secretin (0.75 CU/kg) and the pancreatic juice was collected for an additional 120 minutes.

In vitro measurement of pH_i, $[Ca^{2+}]_i$, $(ATP)_i$, $(\Delta\Psi)_m$, and cAMP. Isolated guinea pig pancreatic ducts or Capan-1 cells were incubated in standard HEPES solution and loaded with BCECF-AM (1.5 μmol/L), Fura2-AM (2.5 μmol/L), Magnesium Green AM (5 μmol/L), or TMRM (100 nmol/L), respectively, for 30 minutes at 37°C. The Transwells or cover glasses were then transferred to a perfusion chamber mounted on an IX71 inverted microscope (Olympus, Budapest, Hungary). The measurements were performed as described previously.[6,15,16] In situ calibration of pH_i in Capan-1 cells (measured with BCECF) was performed using the high K^+-nigericin technique.[17] The initial pH_i of Capan-1 cells was 7.31 ± 0.02. During the experiments, the apical and basolateral membranes of the Capan-1 PDECs were perfused separately, which allowed us to selectively change the composition of the apical or basolateral solutions. The HCO_3^- efflux across the luminal membrane was determined as described previously.[18] Briefly, cells were exposed to 20 mmol/L NH_4Cl in HCO_3^-/co_2-buffered solution from the basolateral and luminal side, which produced an immediate increase in pH_i due to the rapid influx of NH_3 across the membrane. After the alkalization, there was a recovery in pH_i toward the basal value, which depends on the HCO_3^- efflux (ie, secretion) from the duct cells via SLC26 Cl^-/HCO_3^- anion exchanger and CFTR. In this study, the initial rate of recovery from alkalosis (dpH/dt) over the first 30 seconds from the highest pH_i value obtained in the presence of 20 mmol/L NH_4Cl was calculated as described previously.[18] The apical Cl^-/HCO_3^- exchange activity was also measured by using the luminal Cl^- withdrawal technique. Removal of Cl^- from the apical extracellular solution induced an increase in pH_i in PDECs by driving HCO_3^- via the basolateral pNBC1 and the apical SLC26 Cl^-/HCO_3^- exchangers (CBE) into the cells, whereas readdition of Cl^- decreased pH_i, inducing secretion of HCO_3^- via the CBE and the CFTR Cl^- channel. In this study, the rate of pH_i decrease (acidification) after luminal Cl^- readdition was calculated by linear regression analysis of pH_i measurements made over the first 30 seconds after exposure to the Cl^--containing solution.[19] The total buffering capacity ($ß_{total}$) of Capan-1 cells was estimated according to the NH_4^+ pulse technique as described previously.[18]

For $(\Delta\Psi)_m$ measurements, confocal imaging was performed using the FluoView 10i-W system (Olympus). Glass bottom Petri dishes were perfused continuously with solutions containing 100 nmol/L TMRM at 37°C at a rate of 2 to 2.5 mL/min. Five to 10 ROIs (mitochondria) of 5 to 10 cells were excited with light at a given wavelength. Excitation of TMRM was 543 nm, and the emitted light was

captured between 560 and 650 nm to follow the changes of $(\Delta\Psi)_m$.[20]

FRET imaging experiments were performed 24 hours after HEK293 cell transfection with Epac1-camps sensor. Cells were maintained at room temperature in Ringer saline and imaged on an inverted microscope (Olympus IX71) with a 60× NA1.3 oil-immersion objective (Olympus). The microscope was equipped with a charge-coupled device camera (CoolSNAP) and a beam-splitter optical device (Optosplit; Cairn Research, Kent, England). Images were acquired using MetaFluor software (Molecular Devices, Sunnyvale, CA). FRET changes were measured as changes in the background-subtracted 480/545-nm fluorescence emission intensity on excitation at 430 nm and expressed as either R/R0, where *R* is the ratio at time t and *R0* is the ratio at time of 0 seconds, or ΔR/R0, where ΔR = R − R0.

Electrophysiology. Single PDEC and Capan-1 cells were prepared as described previously. A few drops of cell suspension were placed into a perfusion chamber mounted on an inverted microscope (TMS; Nikon, Tokyo, Japan) and allowed to settle for 30 minutes. Patch clamp micropipettes were fabricated from borosilicate glass capillaries (Clark, Reading, England) by using a P-97 Flaming/Brown micropipette puller (Sutter Co, Novato, CA). The resistances of the pipettes were between 2.5 and 4 MΩ. Membrane currents were recorded with an Axopatch1D amplifier (Axon Instruments, Union City, CA) using whole cell at 37°C. After establishing a high-resistance seal (1–10 GΩ) by gentle suction, the cell membrane beneath the tip of the pipette was disrupted. The series resistance was typically 4 to 8 MΩ before compensation (50%–80%, depending on the voltage protocol). Current-voltage relationships were obtained by holding Vm membrane potential at 0 mV and clamping to ±100 mV in 20-mV increments. Membrane currents were digitized by using a 333-kHz analog-to-digital converter (Digidata1200; Axon Instruments) under software control (pClamp6; Axon Instruments). Analyses were performed by using pClamp6 software after low-pass filtering at 1 kHz.[6]

Quantitative real-time reverse-transcription PCR. Total RNA was purified from individual cell culture samples (from 10^6 cells) using the RNA isolation kit of Macherey-Nagel (Düren, Germany). All preparation steps were performed according to the manufacturer's instructions. RNA samples were stored at −80°C in the presence of 30 U Prime RNAse Inhibitor (Thermo Scientific, Szeged, Hungary) for further analysis. The quantity of isolated RNA samples was evaluated by spectrophotometry (NanoDrop 3.1.0; Thermo Fisher Scientific, Rockland, DE). To monitor gene expression, quantitative real-time reverse-transcription PCR was performed on a RotorGene 3000 instrument (Corbett Research, Sydney, Australia) using the TaqMan probe sets of *CFTR* gene (Applied Biosystems). A total of 3 μg of total RNA was reverse transcribed using the High-Capacity cDNA Archive Kit (Applied Biosystems) according to the manufacturer's instructions in a final volume of 30 μL. The temperature profile of the reverse transcription was as follows: 10 minutes at room temperature, 2 hours at 37°C, 5 minutes on ice, and 10 minutes at 75°C for enzyme inactivation in a Thermal Cycler machine (MJ Research, Waltham, MA). After dilution with 30 μL of water, 1 μL of the diluted reaction mix was used as template in the quantitative real-time reverse-transcription PCR. For all reactions, TaqMan Universal Master Mix (Applied Biosystems) was used according to the manufacturer's instructions. Each reaction mixture (final volume, 20 μL) contained 1 μL of primer-TaqMan probe mix. The gene expression assay identification number for CFTR was Hs00357011_m1 and for HPRT was Hs03929098_m1. Quantitative real-time reverse-transcription PCR reactions were performed under the following conditions: 15 minutes at 95°C and 45 cycles of 95°C for 15 seconds and 60°C for 1 minute. Fluorescein dye intensity was detected after each cycle. Relative expression ratios were calculated as normalized ratios to human HPRT internal control gene. A nontemplate control sample was used for each PCR run to check the primer-dimer formation. The final relative gene expression ratios were calculated as ΔCt values (Ct values of gene of interest vs Ct values of the control gene).

Immunofluorescence. *Cultured cells.* For CFTR immunostaining, Capan-1 cells were rinsed twice with phosphate-buffered saline and fixed in 4% paraformaldehyde for 5 minutes at room temperature, followed by 20-minute permeabilization in 0.1% Triton X-100. Nonspecific antibody binding was blocked with 10% goat serum and 1% bovine serum albumin for 60 minutes at room temperature. For detection of CFTR, cells were incubated with anti-NBD2 monoclonal primary CFTR antibody obtained from the CF Foundation (coding no. 596)[21] (1:100) overnight at 4°C. After this, the cells were washed and incubated with anti-mouse fluorescein isothiocyanate conjugated secondary antibody (Dako, Glostrup, Denmark) for 2 hours at room temperature. The nuclei of the cells were stained with Hoechst 33342 (5 μg/mL) for 20 minutes. The images were captured using the FluoView 10i-W system (Olympus).

Guinea pig pancreatic tissue. To detect the effects of ethanol and FA on CFTR expression and localization, we used guinea pig as an in vivo model. The animals were kept at a constant room temperature of 24°C with a 12-hour light-dark cycle and were allowed free access to chow and water. The guinea pigs were treated with a mixture of 0.8 g/kg ethanol (Reanal, Budapest, Hungary) and 300 mg/kg PA intraperitoneally. Before treatment with ethanol and PA, the animals were injected with 1.2 mL physiological saline to avoid ethanol-induced peritoneal irritation. The control animals were treated with 2× 1.2 mL physiological saline intraperitoneally. The animals were killed 3, 6, 12, and 24 hours after injection of pentobarbital (37 mg/kg intraperitoneally) anesthesia. From frozen samples of guinea pig pancreas, 5-μm-thick sections were cut and placed on silanized slides and fixed in 2% paraformaldehyde solution for 15 minutes. After washing in 1% Tris-buffered saline (TBS) solution, slides were stored in 1% bovine serum albumin/TBS for nonspecific antigen blocking. Primary antibody "Mr Pink" (rabbit polyclonal antibody against human CFTR, CFTR Folding Consortium[22,23]) was applied at a dilution of 1:100 in 1% bovine serum albumin/TBS overnight at 4°C and then secondary anti-rabbit antibody (A11034; Alexa Fluor 488;

goat; Invitrogen, Eugene, OR) was used at a dilution of 1:400 for 3 hours at room temperature. Nuclear staining with 4′,6-diamidino-2-phenylindole was performed at a dilution of 1:100 for 20 minutes at room temperature. Between steps, careful TBS washings were applied. Finally, slides were coverslipped with Fluoromount (Dako). RO-density was calculated as described previously.

Detection of CFTR cell surface density, stability, and ER protein folding. *Immunoblotting.* MDCK membrane proteins were solubilized in RIPA buffer (150 mmol/L NaCl, 20 mmol/L Tris-HCl, 1% [wt/vol] Triton X-100, 0.1% [wt/vol] sodium dodecyl sulfate, and 0.5% [wt/vol] sodium deoxycholate, pH 8.0) supplemented with protease inhibitors (10 μg/mL leupeptin and pepstatin, 0.5 mmol/L phenylmethylsulfonyl fluoride) and loaded on a 7% sodium dodecyl sulfate/polyacrylamide gel electrophoresis gel. Immunoblotting was performed with monoclonal anti-HA (Covance, Montreal, Canada) and anti–Na^+/K^+-ATPase (clone H3; Santa Cruz Biotechnology). Densitometry analysis was performed by using ImageQuant TL software (GE Healthcare, London, UK).

Cell surface density and stability measurement of CFTR. The cell surface expression of CFTR-3HA was measured by quantifying the specific binding of mouse anti-HA primary antibody to MDCK cells by enzyme-linked immunosorbent assay as described previously.[24] Cells were seeded in 24-well plates at a density of 8×10^4 cells/well and induced for CFTR-3HA expression. Treatment with ethanol, POA, or POAEE was performed for 48 hours at the indicated concentrations.

Pulse-chase experiments. Experiments were performed as previously described.[25] MDCK cells were cultured as specified and treated previously for 48 hours with ethanol, POA, or POAEE as well as during the pulse and chase periods.

Mouse model of acute alcohol-induced pancreatitis. *Induction of AP.* The mouse model of acute alcohol-induced pancreatitis was originally developed by Huang et al.[26] We modified the original protocol and applied one injection instead of two because the mice tolerated this treatment better. WT and CFTR KO mice were treated with a mixture of 1.75 g/kg ethanol and 750 mg/kg PA intraperitoneally. Before treatment with ethanol and PA, mice were injected with 200 μL physiological saline to avoid ethanol-induced peritoneal irritation. The control mice were treated with 2$\times$ 200 μL physiological saline intraperitoneally. Using the modified protocol, no mortality was observed in the different groups. The mice were killed 24 hours after treatment with ethanol and PA by exsanguination through the heart with pentobarbital (85 mg/kg intraperitoneally) anesthesia. To determine serum amylase activity, blood was collected from the heart. All blood samples were centrifuged at 2500*g* for 15 minutes, and serum was stored at -20°C. The pancreas was quickly removed, trimmed from fat and lymph nodes, and frozen in liquid nitrogen and stored at -80°C until use.

Pancreatic water content. Pancreata were dried for 24 hours at 100°C. Dry weight and wet weight ratio (100 * [wet weight – dry weight]/wet weight) was calculated.

Immunohistochemistry. Pancreatic injury was evaluated by semiquantitative grading of interstitial edema and leukocyte infiltration in a double-blinded manner by 2 independent reviewers. The extent (%) of cell necrosis was confirmed by analysis with ImageJ software as described earlier.[23]

Amylase activity. Serum amylase activity was measured by using a colorimetric kinetic method (Diagnosticum, Budapest, Hungary).

Ethical approvals. *Experiments concerning human subjects.* The scheme of the experiments complies with the ethics of research. It agrees with the declaration of the Medical World Federation proclaimed in Helsinki in 1964. Before enrollment, all volunteers and patients were given a detailed explanation of the nature, possible consequences, and adverse effects of the study by a physician, after which they provided written informed consent. Patients who had temporarily impaired judgment due to the effect of alcohol (patients admitted to the emergency department) were repeatedly given a detailed briefing after they became sober and then gave informed consent again. Unconscious intoxicated patients were not enrolled in this study.

Experiments concerning animals. All experiments were conducted in compliance with the Guide for the Care and Use of Laboratory Animals (National Academies Press, Eight Edition, 2011), with the 2010/63/EU guideline and the Hungarian 40/2013(II.14.) government decree. The experiments were approved by Committees on investigations involving animals at the University of Szeged and also by independent committees assembled by local authorities (XII./3773/2012.).

Supplementary References

1. Raju SV, Jackson PL, Courville CA, et al. Cigarette smoke induces systemic defects in cystic fibrosis transmembrane conductance regulator (CFTR) function. Am J Respir Crit Care Med 2013;88:1321–1330.
2. Yoda T, Crawshaw LI, Nakamura M, et al. Effects of alcohol on thermoregulation during mild heat exposure in humans. Alcohol 2005;36:195–200.
3. Chida K, Takasu T, Kawamura H. Changes in sympathetic and parasympathetic function in alcoholic neuropathy. Nihon Arukoru Yakubutsu Igakkai Zasshi 1998; 33:45–55.
4. Gibson LE, Cooke RE. A test for concentration of electrolytes in sweat in cystic fibrosis of the pancreas utilizing pilocarpine by iontophoresis. Pediatrics 1959; 23:545–549.
5. Watson PE, Watson ID, Batt RD. Prediction of blood alcohol concentrations in human subjects. Updating the Widmark Equation. J Stud Alcohol 1981;42:547–556.
6. Pallagi P, Venglovecz V, Rakonczay Z Jr, et al. Trypsin reduces pancreatic ductal bicarbonate secretion by inhibiting CFTR Cl(-) channels and luminal anion exchangers. Gastroenterology 2011;141:2228–2239 e6.
7. Ratcliff R, Evans MJ, Cuthbert AW, et al. Production of a severe cystic fibrosis mutation in mice by gene targeting. Nat Genet 1993;4:35–41.
8. Xiao F, Li J, Singh AK, et al. Rescue of epithelial HCO_3^- secretion in murine intestine by apical membrane expression of the cystic fibrosis transmembrane conductance regulator mutant F508del. J Physiol 2012; 590:5317–5334.
9. Argent BE, Arkle S, Cullen MJ, et al. Morphological, biochemical and secretory studies on rat pancreatic ducts maintained in tissue culture. Q J Exp Physiol 1986; 71:633–648.
10. Venglovecz V, Hegyi P, Rakonczay Z Jr, et al. Pathophysiological relevance of apical large-conductance Ca(2+)-activated potassium channels in pancreatic duct epithelial cells. Gut 2011;60:361–369.
11. Nikolaev VO, Gambaryan S, Engelhardt S, et al. Real-time monitoring of the PDE2 activity of live cells: hormone-stimulated cAMP hydrolysis is faster than hormone-stimulated cAMP synthesis. J Biol Chem 2005; 280:1716–1719.
12. Cendrowski J, Sanchez-Arevalo Lobo VJ, Sendler M, et al. Mnk1 is a novel acinar cell-specific kinase required for exocrine pancreatic secretion and response to pancreatitis in mice. Gut 2014 Jul 18 [Epub ahead of print].
13. Mensel B, Messner P, Mayerle J, et al. Secretin-stimulated MRCP in volunteers: assessment of safety, duct visualization, and pancreatic exocrine function. AJR Am J Roentgenol 2014;202:102–108.
14. Fernandez-Salazar MP, Pascua P, Calvo JJ, et al. Basolateral anion transport mechanisms underlying fluid secretion by mouse, rat and guinea-pig pancreatic ducts. J Physiol 2004;556:415–428.
15. Venglovecz V, Rakonczay Z Jr, Ozsvari B, et al. Effects of bile acids on pancreatic ductal bicarbonate secretion in guinea pig. Gut 2008;57:1102–1112.
16. Maleth J, Venglovecz V, Razga Z, et al. Non-conjugated chenodeoxycholate induces severe mitochondrial damage and inhibits bicarbonate transport in pancreatic duct cells. Gut 2011;60:136–138.
17. Hegyi P, Rakonczay Z Jr, Gray MA, et al. Measurement of intracellular pH in pancreatic duct cells: a new method for calibrating the fluorescence data. Pancreas 2004; 28:427–434.
18. Hegyi P, Gray MA, Argent BE. Substance P inhibits bicarbonate secretion from guinea pig pancreatic ducts by modulating an anion exchanger. Am J Physiol Cell Physiol 2003;285:C268–C276.
19. Stewart AK, Yamamoto A, Nakakuki M, et al. Functional coupling of apical Cl^-/HCO_3^- exchange with CFTR in stimulated HCO3- secretion by guinea pig interlobular pancreatic duct. Am J Physiol Gastrointest Liver Physiol 2009;296:G1307–G1317.
20. **Baumgartner HK, Gerasimenko JV**, Thorne C, et al. Calcium elevation in mitochondria is the main Ca^{2+} requirement for mitochondrial permeability transition pore (mPTP) opening. J Biol Chem 2009;284: 20796–20803.
21. Kreda SM, Mall M, Mengos A, et al. Characterization of wild-type and deltaF508 cystic fibrosis transmembrane regulator in human respiratory epithelia. Mol Biol Cell 2005;16:2154–2167.
22. **Peters KW, Okiyoneda T**, Balch WE, et al. CFTR Folding Consortium: methods available for studies of CFTR folding and correction. Methods Mol Biol 2011; 742:335–353.
23. **Pallagi P, Balla Z, Singh AK**, et al. The role of pancreatic ductal secretion in protection against acute pancreatitis in mice. Crit Care Med 2014;42:e177–e188.
24. Okiyoneda T, Barriere H, Bagdany MR, et al. Peripheral protein quality control removes unfolded CFTR from the plasma membrane. Science 2010;329:805–810.
25. Rabeh WM, Bossard F, Xu H, et al. Correction of both NBD1 energetics and domain interface is required to restore DeltaF508 CFTR folding and function. Cell 2012; 148:150–163.
26. **Huang W, Booth DM**, Cane MC, et al. Fatty acid ethyl ester synthase inhibition ameliorates ethanol-induced Ca^{2+}-dependent mitochondrial dysfunction and acute pancreatitis. Gut 2014;63:1313–1324.

Author names in bold designate shared co-first authorship.

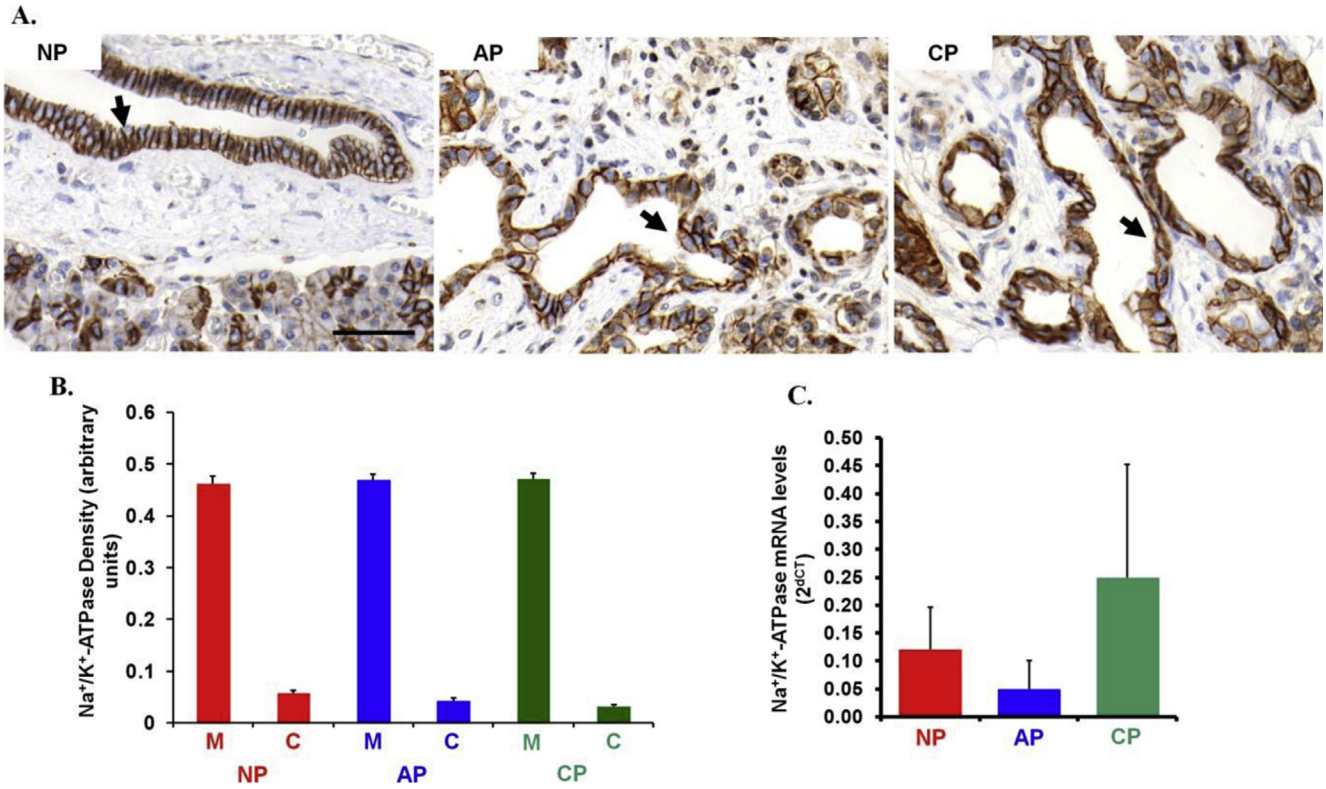

Supplementary Figure 1. Expression of Na^+/K^+-ATPase in human pancreas is not changed in AP or CP. (*A*) Na^+/K^+-ATPase expression in human pancreas. *Arrows* point to the pancreatic ducts. NP, normal pancreas. *Scale bar* = 50 μm. (*B*) Relative density of Na^+/K^+-ATPase. The density of Na^+/K^+-ATPase staining was not changed. C, cytoplasm; M, membrane. n = 5. (*C*) Quantitative PCR analysis of Na^+/K^+-ATPase mRNA expression in the human pancreas. Na^+/K^+-ATPase mRNA levels were not changed significantly. Data were normalized to 18 ribosomal RNA and given as a percentage of NP mRNA levels. n = 5.

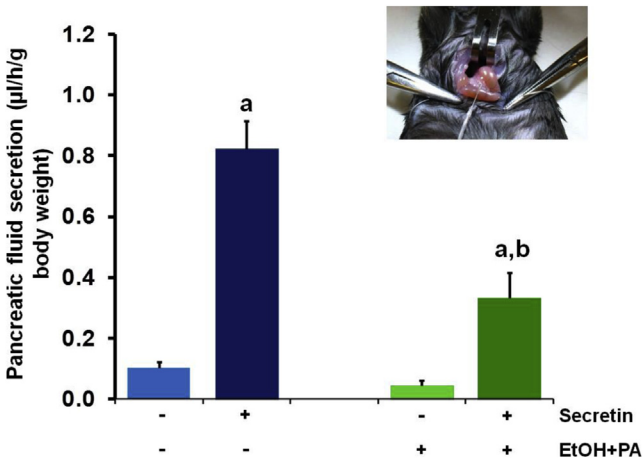

Supplementary Figure 2. Ethanol and fatty acids inhibit pancreatic fluid secretion. In vivo pancreatic fluid secretion was directly measured in anesthetized mice. Intraperitoneal injection of ethanol and PA significantly decreased both basal (0.102 ± 0.02 μL/h/g body weight vs 0.045 ± 0.016 μL/h/g body weight) and secretin-stimulated (0.824 ± 0.092 μL/h/bwg vs 0.334 ± 0.082 μL/h/g body weight) pancreatic fluid secretion. n = 6/group. $^aP < .001$ vs control before secretion stimulation, $^bP < .001$ vs secretin-stimulated untreated group.

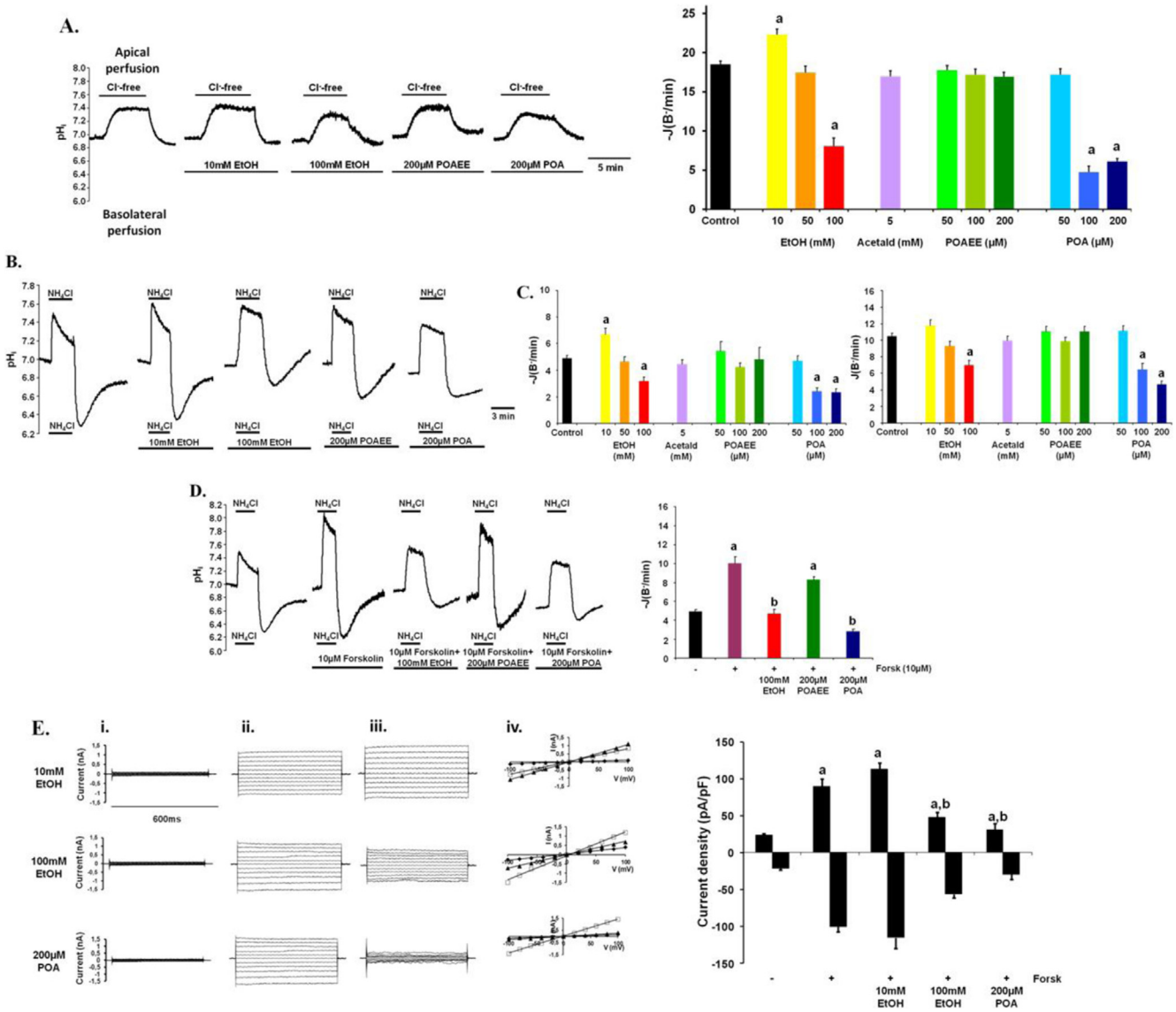

Supplementary Figure 3. (*A*) Representative pH_i traces and summary data of the initial rate of recovery after readdition of Cl^- showing the effect of basolateral administration of ethanol, acetaldehyde, POAEE, and POA for 15 minutes on pH_i recovery in Capan-1 pancreatic ductal cells. Cells were perfused separately from the apical and basolateral side with co_2/HCO_3^- buffered solution. *Labels above the traces* indicate the Cl^- composition of the luminal solution, and *labels below the traces* denote test compounds added to basolateral perfusion solution. Administration of 10 mmol/L ethanol significantly stimulated the activity of the luminal transporters. On the other hand, 100 mmol/L ethanol and 100 to 200 μmol/L POA significantly inhibited recovery. Data are shown as means ± SEM. n = 3 to 5 experiments for all groups. $^aP < .05$ vs control. (*B–D*) Representative pH_i traces and summary data of the initial rate of recovery from alkali and acid load under resting and stimulated conditions. Alkali and acid load was induced by 20 mmol/L NH_4Cl in HCO_3^-/co_2 buffered solution in Capan-1 cells. A total of 10 mmol/L ethanol stimulated whereas 100 mmol/L ethanol and high concentrations of POA significantly inhibited the activity of luminal (*C* [*left panel*], recovery from alkali load) and basolateral transporters (*C* [*right panel*], recovery from acid load) and forskolin-stimulated secretion (*D*), respectively. Data are shown as means ± SEM. n = 3–5 experiments for all groups. $^aP < .05$ vs control, $^bP < .05$ vs 10 microM Forsk. (*E*) Representative fast whole cell CFTR Cl^- current recordings from Capan-1 cells. (*i*) Unstimulated currents, (*ii*) currents after 10-minute stimulation with 10 μmol/L forskolin, (*iii*) stimulated currents after 10-minute exposure to 10 mmol/L or 100 mmol/L ethanol and 200 μmol/L POA, and (*iv*) current-voltage relationships (*diamonds* represent unstimulated currents, *squares* represent forskolin-stimulated currents, and *triangles* represent forskolin-stimulated currents in the presence of the tested agents). Summary of the current density (pA/pF) measured at reversal potential ± 60 mV. Exposure of Capan-1 cells to 10 mmol/L ethanol stimulated but 100 mmol/L ethanol or 200 μmol/L POA blocked the forskolin-stimulated CFTR Cl^- currents. n = 5–6 for all groups. $^aP < .05$ vs basal current, $^bP < .05$ vs forskolin-stimulated current.

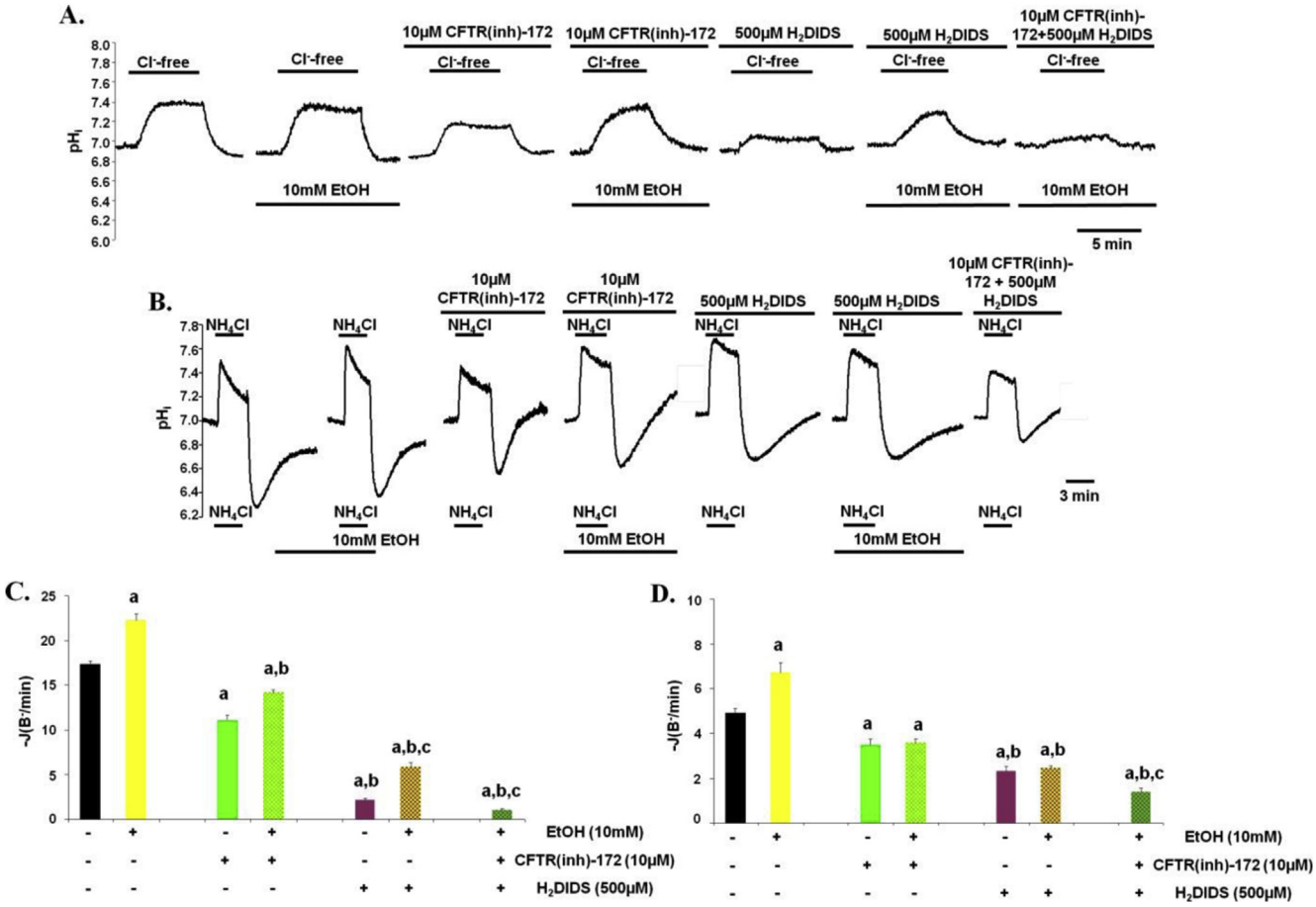

Supplementary Figure 4. A low concentration of ethanol stimulates the luminal CBE and CFTR in Capan-1 PDECs. Representative pH_i traces showing the effect of luminal administration of 500 μmol/L H_2DIDS and/or 10 μmol/L CFTR(inh)-172 in the presence or absence of 10 mmol/L ethanol on pH_i recovery after (*A*) Cl^- readdition or (*B*) after alkali load. (*C*) Summary data of the initial rate of pH_i recovery after readdition of chloride. Administration of 10 μmol/L CFTR(inh)-172 and 500 μmol/L H_2DIDS inhibited recovery. Ethanol (10 mmol/L) stimulated recovery in both cases. The combined administration of CFTR(inh)-172 and H_2DIDS abolished the stimulatory effect. These data suggest that low concentrations of ethanol stimulate activity of CBE and CFTR on the apical membrane of PDECs. (*D*) Summary data of the initial rate of pH_i recovery after alkali load. Administration of 10 μmol/L CFTR(inh)-172 and 500 μmol/L H_2DIDS inhibited recovery. However, 10 mmol/L ethanol failed to stimulate recovery under these circumstances. Data are shown as means ± SEM. n = 3–5 experiments for all groups. $^aP < .05$ vs control, $^bP < .05$ vs 10 μmol/L CFTR(inh)-172, $^cP < .05$ vs 500 μmol/L H_2DIDS.

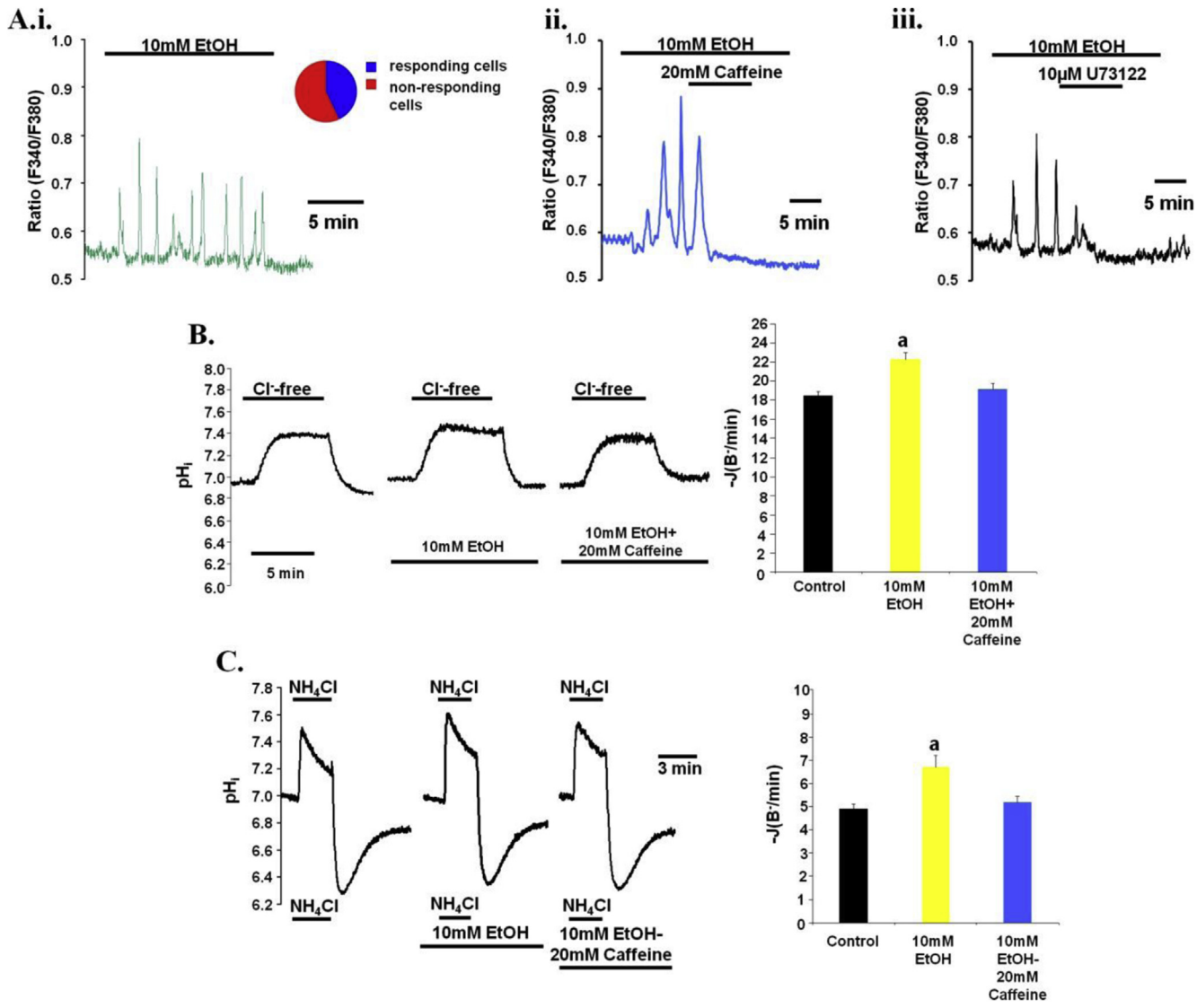

Supplementary Figure 5. The stimulatory effect of 10 mmol/L ethanol is mediated by elevation of $[Ca^{2+}]_i$. (*A*) Representative curves show the effect of low concentrations of ethanol on the $[Ca^{2+}]_i$ of PDECs. (*i*) Administration of 10 mmol/L ethanol induced short-lasting, repetitive Ca^{2+} spikes in 43% of the cells. The Ca^{2+} oscillation induced by 10 mmol/L ethanol was abolished by (*ii*) 20 mmol/L caffeine and (*iii*) 10 μmol/L U73122. (*B*) Representative curve and summary data show the effect of pretreatment with caffeine on ethanol-stimulated apical Cl^-/HCO_3^- exchange activity. Caffeine abolished the stimulatory effect of low concentrations of ethanol. (*C*) Representative traces and summary data show the effect of administration of caffeine on HCO_3^- secretion of PDECs. Pretreatment with caffeine abolished the stimulatory effect of 10-minute administration of low concentrations of ethanol on HCO_3^- secretion. Data are shown as means ± SEM. n = 3–5 experiments for all groups. $^aP < .05$ vs control.

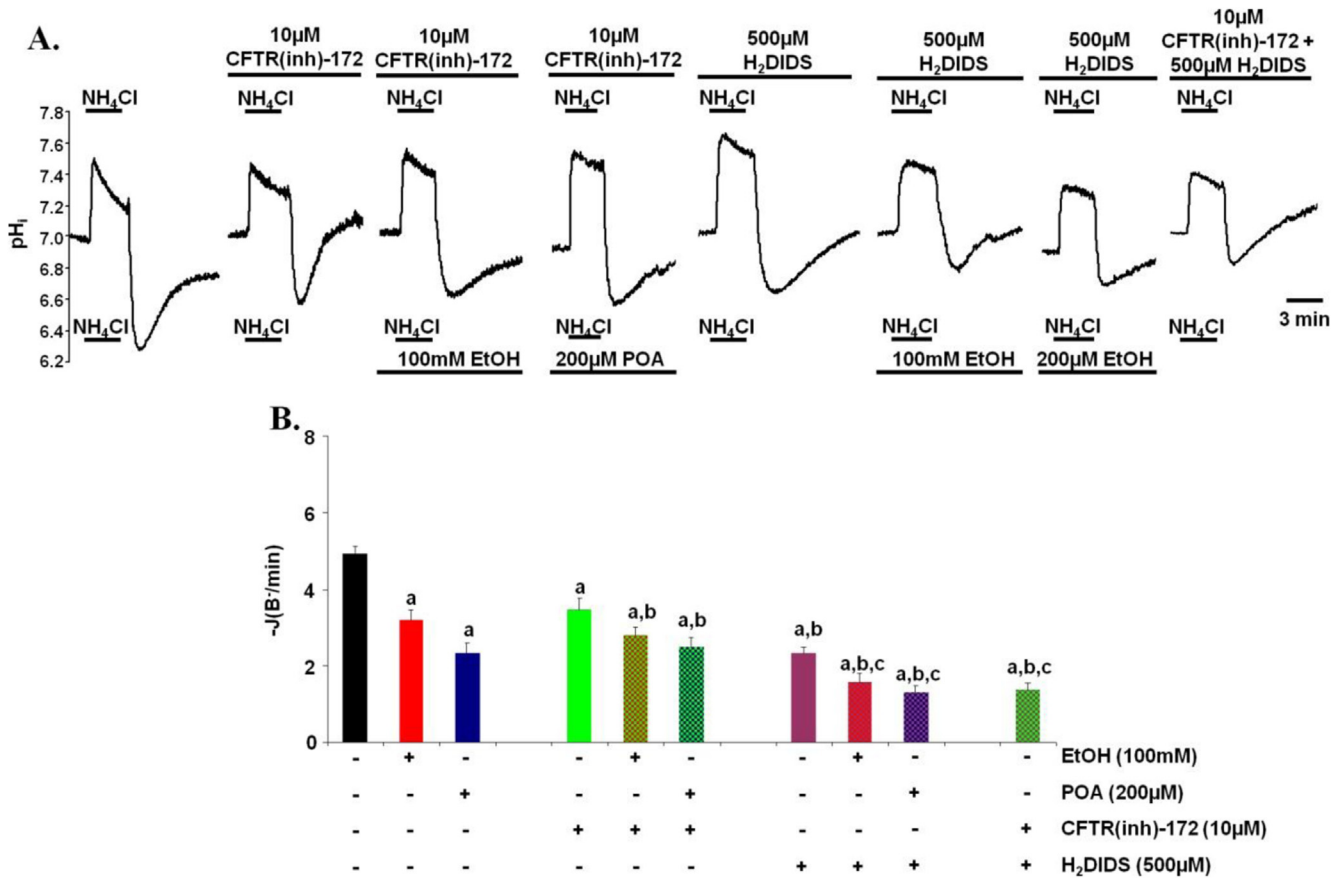

Supplementary Figure 6. High concentrations of ethanol and fatty acids inhibit luminal CBE and CFTR in Capan-1 PDECs. (*A*) Representative pH_i traces of the effects of basolateral administration of 100 mmol/L ethanol or 200 μmol/L POA for 10 minutes in the presence or absence of 500 μmol/L H_2DIDS and/or 10 μmol/L CFTR(inh)-172 (luminal administration) on pH_i recovery after alkali load in HCO_3^-/co_2-buffered solution. (*B*) Summary data of the initial rate of pH_i recovery after alkali load. Our results further confirmed the inhibitory effect of ethanol and POA on CBE and CFTR. Data are shown as means ± SEM. n = 3–5 experiments for all groups. $^aP < .05$ vs control, $^bP < .05$ vs 10 μmol/L CFTR(inh)-172, $^cP < .05$ vs 500 μmol/L H_2DIDS.

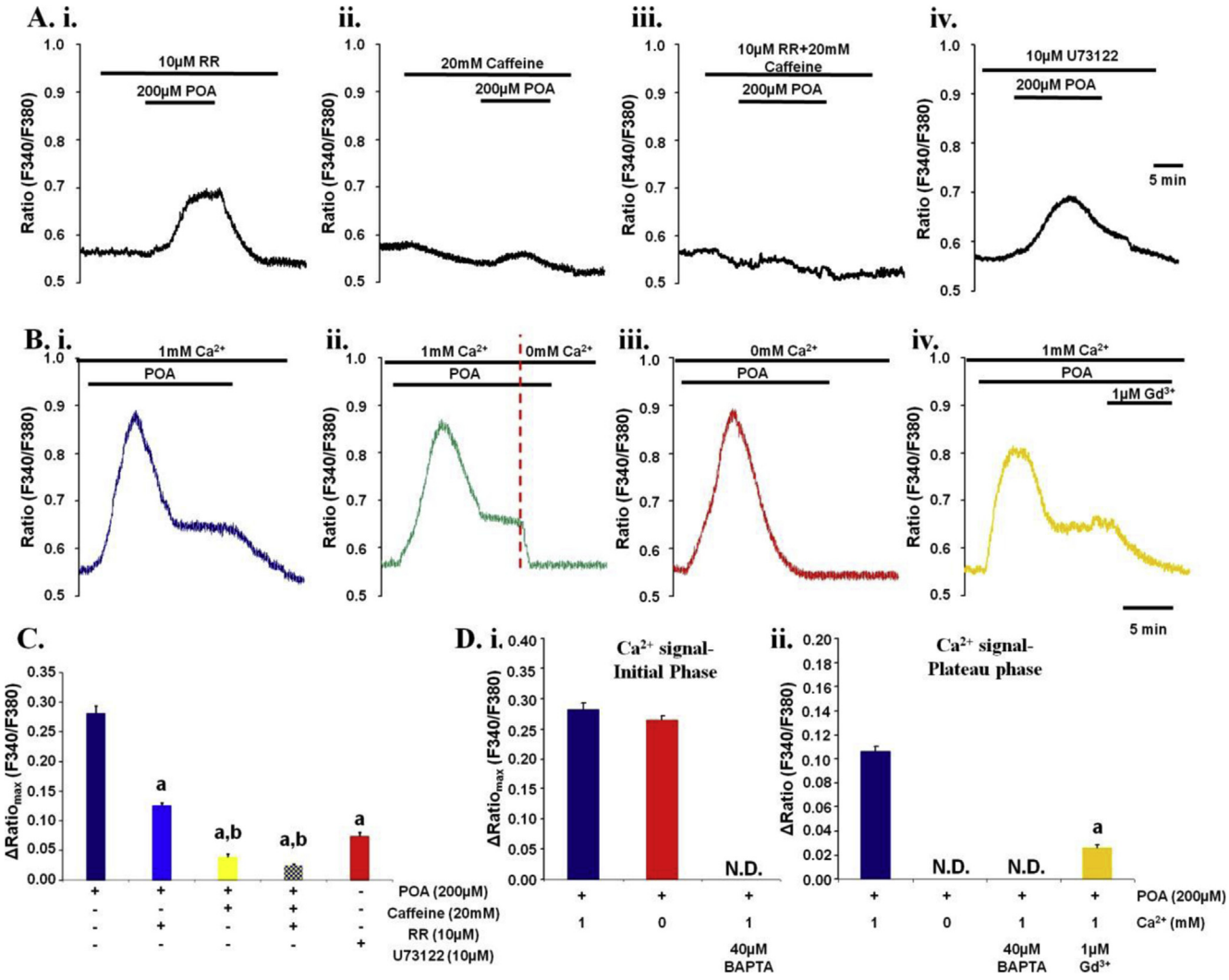

Supplementary Figure 7. (*A*) POA releases Ca^{2+} from the ER via IP_3R and ryanodine receptor activation in Capan-1 PDECs. Representative curves show the effect of IP_3R and ryanodine receptor inhibition on Ca^{2+} release induced by 200 μmol/L POA. Administration of (*i*) 10 μmol/L Ruthenium Red significantly decreased the effect of POA on $[Ca^{2+}]_i$ (55.5%), and (*ii*) administration of 20 mmol/L caffeine induced significantly higher inhibition (86.1%). (*iii*) The combined administration of RR and caffeine did not induce further inhibition (92.1%). (*iv*) The PKC inhibitor U73122 decreased the effect of POA similarly to caffeine (73.5%). (*B*) The plateau phase of the POA-induced Ca^{2+} signal depends on extracellular Ca^{2+} influx. Representative curves show the effect of the administration of (*i*) 200 μmol/L POA on $[Ca^{2+}]_i$. (*ii*) Removal of extracellular Ca^{2+} during the plateau phase of the Ca^{2+} signal abolished the elevation of Ca^{2+}. (*iii*) The plateau phase was completely absent in Ca^{2+}-free extracellular solution and (*iv*) was significantly inhibited by administration of 1 μmol/L Gd^{3+}. (*C*) Summary data of the $\Delta Ratio_{max}$. The administration of RR, caffeine, and U73122 significantly decreased the effect of POA on $[Ca^{2+}]_i$. Data are shown as means ± SEM. n = 3–5 experiments for all groups. $^aP < .05$ vs control, $^bP < .05$ vs 10 μmol/L RR. (*D*) (*i*) Summary data of the $\Delta Ratio_{max}$ of the initial phase of the POA-induced Ca^{2+} signal. The effect of POA on the $\Delta Ratio_{max}$ was not affected by extracellular Ca^{2+} withdrawal. Pretreatment with 40 μmol/L BAPTA-AM for 30 minutes completely abolished the elevation of Ca^{2+}. (*ii*) Summary data of the ΔRatio of the plateau phase of the POA-induced Ca^{2+} signal. The plateau phase of the POA-induced Ca^{2+} signal was completely based on extracellular Ca^{2+} influx. Data are shown as means ± SEM. n = 3–5 experiments for all groups. N.D., not detected. $^aP < .05$ vs initial phase, $^bP < .05$ vs plateau phase.

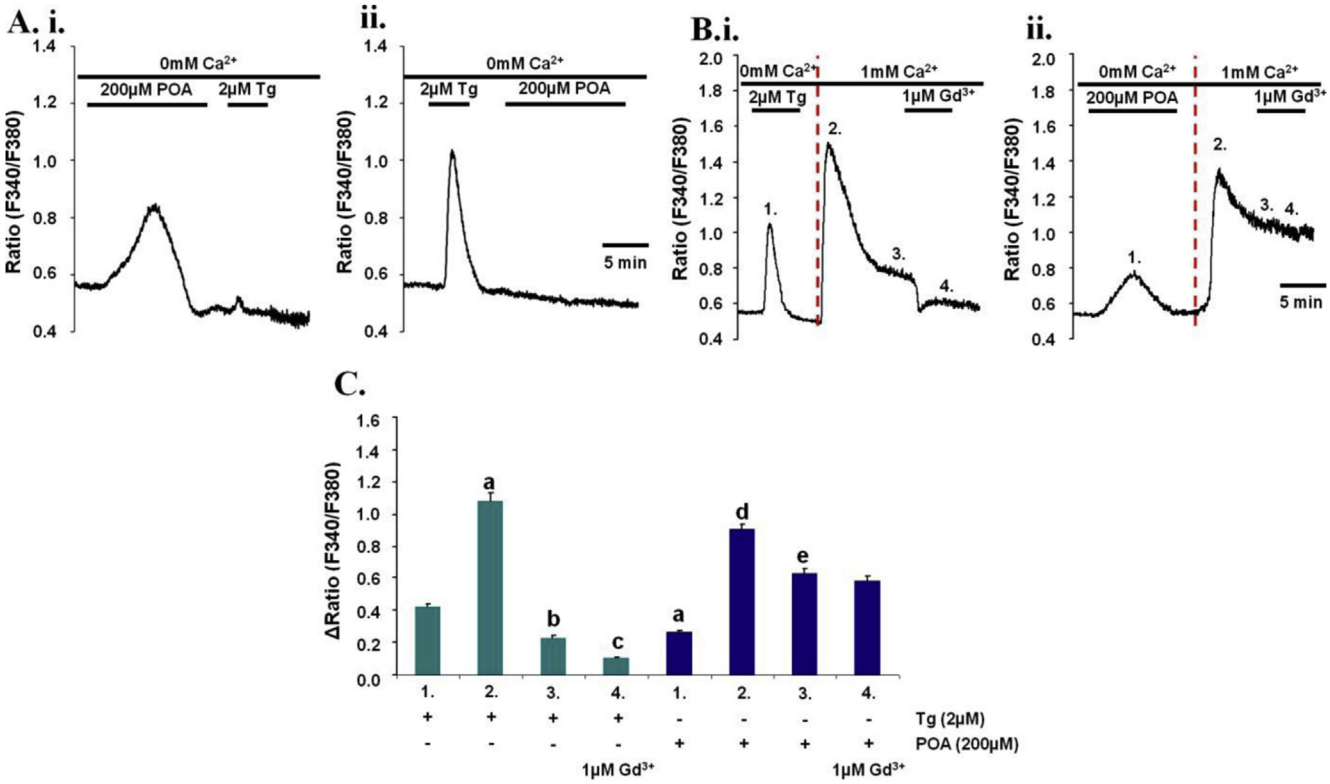

Supplementary Figure 8. (*A*) Administration of 200 μmol/L POA completely depletes ER Ca^{2+} stores. (*i*) After administration of 200 μmol/L POA, the SERCA inhibitor Tg was not able to induce further Ca^{2+} release. (*ii*) Similarly, POA was not able to induce further Ca^{2+} release after Tg administration. (*B* and *C*) Administration of 200 μmol/L POA induces store-operated extracellular Ca^{2+} influx. (*i*) Administration of 2 μmol/L Tg in Ca^{2+}-free extracellular solution depleted the ER Ca^{2+} store (1). Readdition of extracellular Ca^{2+} induced rapid elevation of $[Ca^{2+}]_i$ (2), which was followed by a decrease and an equilibrium (3). Gd^{3+} significantly decreased Ca^{2+} influx (4). Administration of 200 μmol/L POA in Ca^{2+}-free extracellular solution also depleted the ER Ca^{2+} store (1), which was followed by elevation of $[Ca^{2+}]_i$ after readdition of extracellular Ca^{2+} (2). The decrease after the maximal Ca^{2+} elevation was slower than in the case of the Tg-treated cells, and the equilibrium was reached on an elevated $[Ca^{2+}]_i$ level (3), which suggest the failure of the plasma membrane Ca^{2+} ATPase (PMCA). Gd^{3+} had no effect on the Ca^{2+} influx in this case (4). $^{a}P < .05$ vs 2 μmol/L Tg 1, $^{b}P < .05$ vs 2 μmol/L Tg 2, $^{c}P < .05$ vs 2 μmol/L Tg 3, $^{d}P < .05$ vs 200 μmol/L POA 1, $^{e}P < .05$ vs 200 μmol/L POA 2.

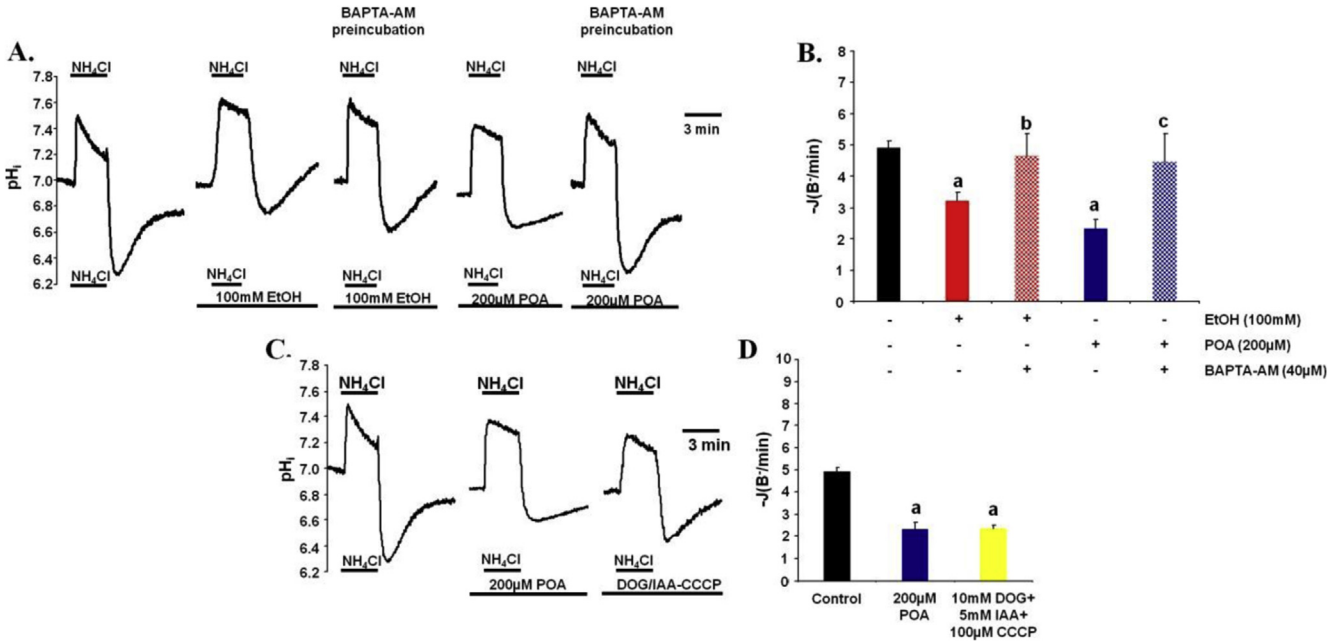

Supplementary Figure 9. (*A*) $[Ca^{2+}]_i$ chelation abolishes the inhibitory effect of ethanol and POA on pancreatic HCO_3^- secretion in Capan-1 PDECs. Representative traces showing the effect of Ca^{2+} chelation on the inhibitory effect of 100 mmol/L ethanol or 200 μmol/L POA on recovery after alkali load. (*B*) Summary data of the initial rate of pH_i recovery after alkali load. The chelation of $[Ca^{2+}]_i$ abolished the inhibitory effect of ethanol and POA on HCO_3^- secretion. Data are shown as means ± SEM. n = 3–5 experiments for all groups. $^aP < .05$ vs control, $^bP < .05$ vs 100 mmol/L ethanol, $^cP < .05$ vs 200 μmol/L POA. (*C*) The effect of $(ATP)_i$ depletion on HCO_3^- secretion. Representative traces show the effect of $(ATP)_i$ depletion on HCO_3^- secretion. Administration of 10 mmol/L DOG, 5 mmol/L IAA, and 100 μmol/L CCCP significantly inhibited the recovery after alkali load. (*D*) Summary data of the recovery after alkali load. The recovery after alkali load was significantly reduced by $(ATP)_i$ depletion. Data are shown as means ± SEM. n = 3–5 experiments for all groups. $^aP < .05$ vs control.

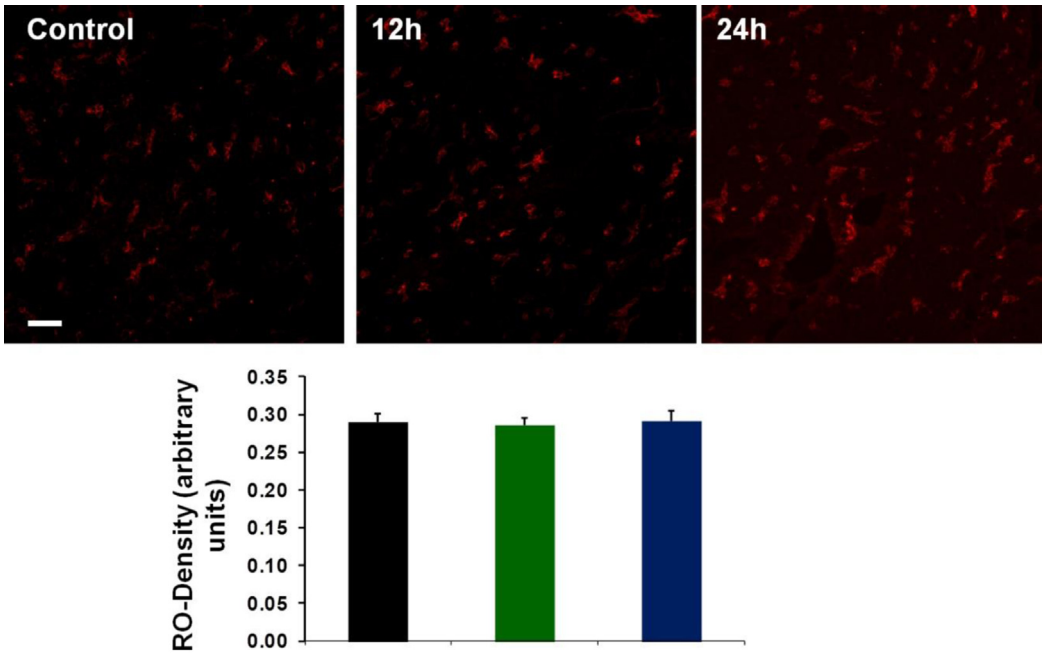

Supplementary Figure 10. Na^+/K^+-ATPase expression in guinea pig pancreas. The expression of Na^+/K^+-ATPase of guinea pig pancreatic ducts did not change after a single intraperitoneal injection of 0.8 g/kg ethanol and 300 mg/kg PA. n = 5 for each group. $P < .05$ vs control. *Scale bar* = 100 μm. Data are shown as means ± SEM.

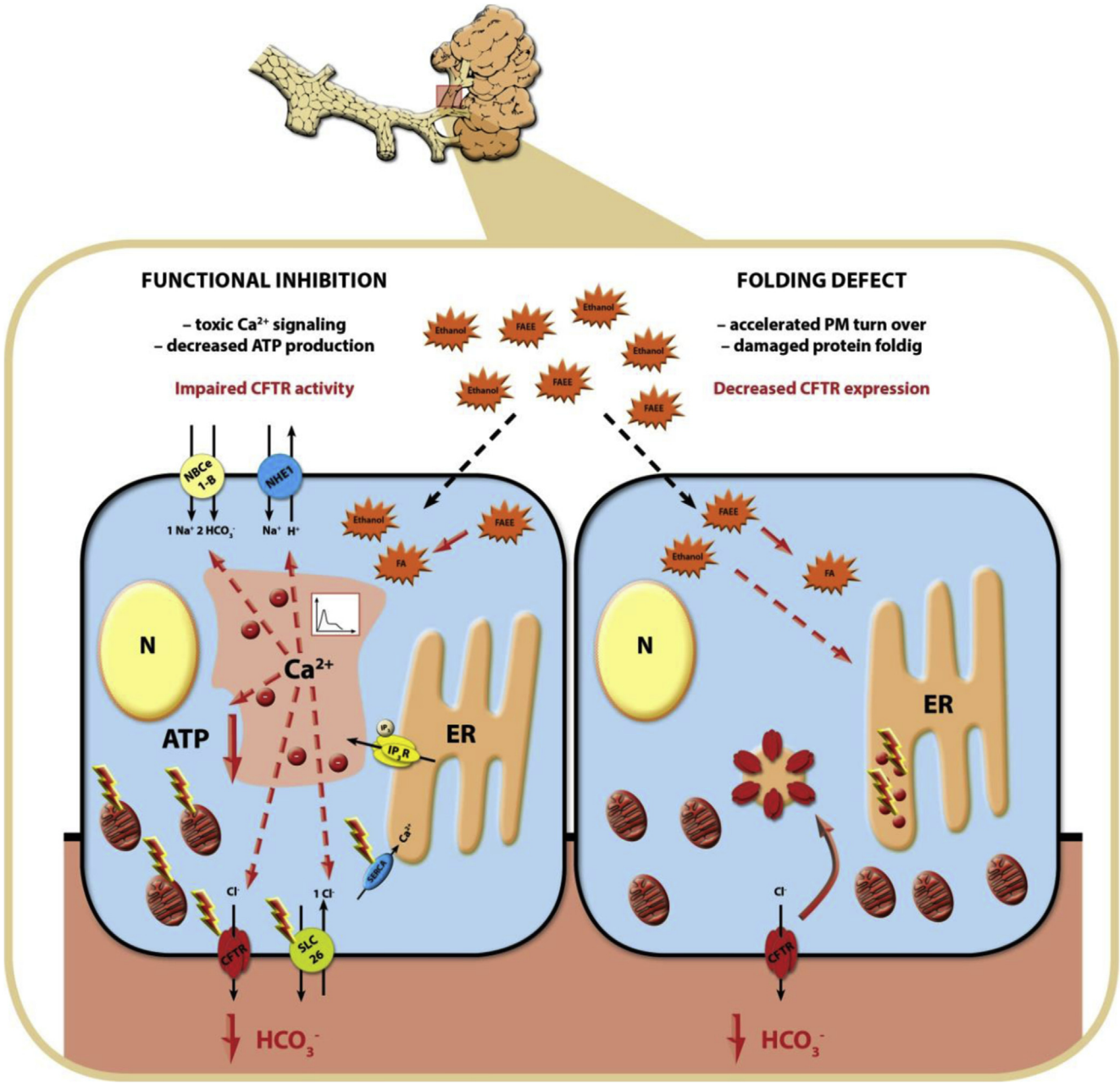

Supplementary Figure 11. Ethanol and nonoxidative ethanol metabolites induce sustained intracellular calcium overload, cellular cAMP and ATP depletion, and mitochondrial membrane depolarization in pancreatic ductal epithelial cells. These events inhibit CFTR activity and decrease pancreatic HCO_3^- secretion. On the other hand, ethanol and nonoxidative ethanol metabolites severely reduce CFTR expression via a combination of reduced CFTR mRNA levels, decreased cell surface stability, and ER folding defect of CFTR. The decreased pancreatic fluid and HCO_3^- secretion will increase the severity of alcohol-induced acute pancreatitis.